Physics – Uspekhi **42** (4) 297 – 319 (1999)

REVIEWS OF TOPICAL PROBLEMS PACS numbers: **61.43.–j**, 61.43.Er, **66.30.–h**

Diffusion mechanisms in disordered systems: computer simulation

D K Belashchenko

Contents

Abstract. Computer simulation results on diffusion in metal and some nonmetal amorphous materials are summarized. Methods for producing and analyzing disordered systems as well as for modeling diffusion processes in such systems are considered. Certain features of diffusion in disordered systems are demonstrated. Possible mechanisms of diffusion in amorphous metals are analyzed.

1. Introduction

Modern ideas about the mechanism of diffusion in simple liquids were formulated in the 1960s basically by computer simulation methods, the molecular dynamics method and the Monte Carlo method. The situation with amorphous systems proved to be more complicated. Not so long ago even the possible mechanisms of diffusion processes in amorphous systems were unclear. The very notion of a vacancy (or quasivacancy) was debatable. Lately, however, the understanding of the nature and mechanisms of diffusion processes in disordered systems has substantially improved because of the wide use of computer simulation methods. Studying atomic models, one can extract much more information about the behavior at the atomic level than real experiments can provide.

D K Belashchenko Moscow Institute of Steel and Alloys (Technological University), Leninskiĭ prosp. 4, 117936 Moscow, Russian Federation
Tel. (7-095) 230 46 67
Fax (7-095) 237 80 07
E-mail: dkbel@bel.misa.ac.ru

Received 25 February 1998, revised 15 June 1998
Uspekhi Fizicheskikh Nauk **169** (4) 361 – 384 (1999)
Translated by E Yankovsky; edited by S D Danilov

Usually diffusion mobility in real amorphous media (glasses) is very low, since such systems become unstable and crystallize at moderate temperatures. By analogy with diffusion in crystalline materials we can assume that there are activation mechanisms of diffusion in glasses. For instance, for hydrogen dissolved in an amorphous alloy, the activation mechanism of diffusion along the interstices of the amorphous matrix may come into play. Such a mechanism is less probable for bigger atoms, and other mechanisms for which the hopping mode of particle transport is a characteristic feature (this mode is related to surmounting the activation barrier) should be considered.

On the other hand, since the amorphous phase can be reached by cooling the liquid, it is natural to take into account the diffusion mechanisms characteristic of liquids. The diffusion mechanism in simple liquids is cooperative ('drift') since it is realized through the simultaneous small displacements of a large number of particles. We must establish whether this mechanism provides a sizable contribution to diffusion when the liquid is moderately or deeply supercooled, down to temperatures at which the liquid becomes an amorphous substance, and in the amorphous phase proper.

The experimental possibilities of analyzing the diffusion mechanisms in supercooled liquids and amorphous systems are limited. Under diffusion annealing, the particles of the amorphous system usually travel over distances of several atomic separations, a maximum several tens of separations (with the exception of solutions of hydrogen in amorphous alloys, where the impurity mobility is high). Hence much attention is focused on the theoretical analysis of diffusion processes by analytical methods or computer simulation.

Measurements of diffusion characteristics in amorphous systems are hindered by the fact that in the process of

diffusion annealing structure relaxation is always present to a certain extent, which leads to 'defect healing,' 'free-volume outflow,' etc. It was found, for instance, that when hydrogen and deuterium diffuse in the amorphous alloy $Co_{76.7}Fe_2Nb_{14.3}B_7$, structure relaxation changes the isotopic effect severalfold [1]. 'Free-volume outflow' is always realized with direct participation of diffusion processes. For instance, in amorphous alloys of cobalt, copper, or nickel, the activation energies of diffusion and free-volume outflow are extremely close [2].

Recently several reviews on diffusion in amorphous alloys have been published (e.g., see Refs [3 – 7]). It has been found that it is extremely difficult to draw any conclusions about the diffusion mechanisms in amorphous systems because of the diversity of objects and substantial discrepancies in the experimental data. And yet, according to Larikov [6], several experimental results can be considered as being established with a greater or lesser certainty. The kinetics and mechanisms of diffusion in amorphous metal alloys (AMA) are closer to imperfect crystals than to liquids. The rate of diffusion of metal atoms in AMA is higher, and that of metalloid atoms is lower, than in perfect crystals of the base metal (or solid solution based on the metal), but it is lower for the metal atoms in comparison to a crystallized alloy of the same composition as the AMA. The reason is that in crystallized alloys the structure is finely granular and diffusion primarily proceeds along the interface, where the diffusion coefficients are larger than in AMA. In different AMA of the metal – metalloid type, the diffusion of the same elements proceeds at close rates at equal relative temperatures T/T_g, where T_g is the glass transition (vitrification) temperature.

It is assumed that small atoms (B, Si, and C) diffuse along 'quasi-interstices' and larger atoms, along 'quasivacancies.' The diffusion coefficients for small atoms are much larger than for large atoms. No simple relationships that describe the diffusion coefficients for the different components in metal – metal AMA have been discovered.

A characteristic feature of solutions of hydrogen in AMA is the presence of quasi-interstices with different energies of bonding with hydrogen atoms. The first portions of hydrogen are captured more strongly and diffuse more slowly. Hence the diffusion coefficient is concentration-dependent and obeys a temperature law of the Arrhenius type, and instead of random-walk theory one is forced to use percolation theory.

The computer simulation method is covered rather scantily in the above-mentioned reviews on diffusion in disordered systems. However, these methods make it possible to study in great detail and from a unified standpoint the possible mechanisms of diffusion in disordered systems of various types, e.g. in systems with different types of chemical bond. The goal of the present review is the analysis and systematization of the data on mechanisms of diffusion in disordered systems obtained by computer simulation. We will briefly discuss the methods of constructing models of liquid and amorphous systems, the interparticle interaction potentials used in these methods, and the various algorithms of studying diffusion in the models. We will also analyze the main mechanisms of diffusion in liquids and amorphous phases, the cooperative (drift) and the activation. Using examples of disordered lattices, we will expose the role of the energy distributions of the stable and transition states in the case of activated diffusion. The mechanism of diffusion along interstices in the amorphous phases will be examined (the diffusion of hydrogen and carbon, in particular). Finally, we will present an overview of the problem of defects in amorphous bodies, especially pores (quasivacancies) and will discuss their role in diffusion processes.

Sections 2 – 6 deal primarily with dense disordered systems, such as metal alloys and simple salt systems. Systems with a loose structure, covalent (of the type of amorphous silicon) and ionic-covalent (of the silica type), differ from the above systems substantially. Computer data on the mechanisms of diffusion in loose systems are discussed in Section 7.

2. Methods of constructing computer models of disordered systems

The methods most often used in constructing models are those of static relaxation, molecular dynamics, and Monte Carlo and a group of methods that use diffraction data on the structure of the system. To construct models by the methods of static relaxation (at absolute zero), molecular dynamics, and Monte Carlo (at finite temperatures) one must initially specify the potentials of interparticle interaction. The other group of methods only uses data on the density of the system and the pair correlation functions extracted from the data of diffraction experiments.

In the classical (nonquantum) variant of the Monte Carlo method, the particles of the model are successively shifted (in a virtual manner) in a direction taken at random over a small distance (step), the change ΔU in the potential energy of the system is calculated, and event drawing is done by comparing $w = \exp(-\Delta U/kT)$ and a random number A: $0 < A < 1$ [8, 9]. If $\Delta U < 0$ or A is smaller than w, the displacement is accepted, otherwise it is rejected. Conducting a long sequence of particle displacements, we obtain a large set (usually millions) of realizations of the system that obey Gibbs statistics, and using this set we can calculate the structural characteristics of the system and any of the thermodynamic properties, such as energy, pressure, and entropy. If the data gathered in this manner agree with the experimental data, the interparticle potentials have been chosen correctly. Time does not enter into the method explicitly, so that it is impossible to directly calculate the transport characteristics of the system, e.g. diffusion coefficients.

For large systems, periodic boundary conditions are usually introduced. The particles are placed inside the main cube, which is translated along the three axes of coordinates together with the particles inside it, which results in the formation of a simple cubic superlattice. The particles can interact with their neighbors in the main cube and in the neighboring cubes.

The static relaxation and molecular dynamics methods involve calculating the paths of the particles under forces. In the static relaxation method the system is at absolute zero, there is no kinetic energy, and the particles are displaced in the direction in which the resultant force acts. The length of the displacement (the step) can be controlled in different ways. In the continuous static relaxation method [10], the step is the same for all the particles, but in the process of relaxation it gradually decreases to a value of the order of zero-point vibrations. The displacement step in the Haimendal algorithm is proportional to the resultant force. In the latter case the probability of the system landing in a local energy minimum is high, so that the system becomes 'jammed.' The algorithm of continuous static relaxation is to a great extent

free from this drawback and is especially useful for constructing models of amorphous systems. However, it has the same drawback as the Monte Carlo method: the displacements of particles do not take place on a real time scale.

The molecular dynamics method [11–14] makes it possible to model particle paths in real time by using the equations of classical dynamics. For instance, good results are produced by applying the simple Verlet algorithm, in which the coordinate of the ith particle in the next, $(k+1)$st step is calculated from the coordinates in the given kth step and the previous $(k-1)$st step:

$$\mathbf{r}_i(k+1) = 2\mathbf{r}_i(k) - \mathbf{r}_i(k-1) + \frac{\mathbf{F}_i(k)(\Delta t)^2}{m}. \quad (1)$$

Here $\mathbf{r}_i$ is the radius vector of the particle, m is the particle mass, $\mathbf{F}_i$ is the resultant force on the particle, and Δt is size of the step on the time scale. The particle velocity is not present in path calculations. The self-diffusion coefficient can be calculated from the mean square of the displacement of the model particles over a large number of steps. Other algorithms of path calculations are discussed in the monograph of Polukhin et al. [14].

The key issue in this method is the calculation of the forces. The common potentials used in modeling simple liquids (of the argon type) and metallic single- and multicomponent systems are short-range pair interparticle potentials (e.g. Lennard-Jones and Morse potentials) containing adjustable parameters. Here, to reduce the computer time, the potential is cut off at a relatively small distance. For ionic systems with a long-range Coulomb interaction the potential cannot be cut off and in calculating the forces one must employ the Ewald procedure, which allows for the interaction between the particles in the main cube and the image cubes [13]. Computer times increase substantially for such calculations.

When modeling systems with a covalent bond, one is forced to introduce, in addition to the pair interaction, three-body interaction potentials, which incorporate particle separations and the values of the valence bands. In this case the potential energy of the system can be written as

$$U(r) = \sum_{i<j} u_{ij}(r) + \sum_{i,j,k} \varphi_{ijk}(\mathbf{r}_i, \mathbf{r}_j, \mathbf{r}_k). \quad (2)$$

Here the functions u_{ij} represent the pair contributions to the energy, which, in principle, resemble, e.g. the Lennard-Jones potential (as in argon), and the second sum represents three-body contributions. The angular dependence of the potential can be described, say, by introducing $(\cos\theta - \cos\theta_0)^2$ type factors, where θ is the actual valence angle for a triplet of atoms, and θ_0 is the equilibrium value of this angle (e.g. 109.5° for a tetrahedral configuration).

The potentials most often used to describe three-body interaction are the Axilrod–Teller, Keating, and Stillinger–Weber potentials [13, 15]. The Stillinger–Weber potential, first proposed for silicon, is written

$$\varphi_{ijk} = \lambda \exp\left[\gamma(r_{12}-a)^{-1} + \gamma(r_{13}-a)^{-1}\right]\left(\cos\theta + \frac{1}{3}\right)^2. \quad (3)$$

Here r_{12} and r_{13} are the distances from the central atom (*1*) to each of its neighbors (*2* and *3*) (these distances must be smaller than a), θ is the angle between the vectors $\mathbf{r}_{12}$ and $\mathbf{r}_{13}$, and a, λ, and γ are adjustable parameters. The presence of an angular factor leads to stabilization of the tetrahedral valence angle 109.5°, for which $\cos\theta = -1/3$. The Stillinger–Weber potential was used to model tetrahedral semiconductors (silicon and germanium) and liquid and amorphous carbon and fullerene [16]. The computer time needed to calculate covalent models is much longer than in the case with pair interactions.

Nevertheless, modern computers make it possible to construct fairly large models. For instance, Holender and Morgan [17] used the method of combining small blocks to construct a model of amorphous silicon consisting of 110592 particles, and Nakano et al. [18] constructed ionic models of liquid and glassy silica (with allowance for three-body contributions to the potential) consisting of 41472 particles. The main cube in such a model has an edge 8.5-nm long. A parallel computer with eight processors was used for the calculations, and data was extracted not only about short-range order but also about what is known as medium-range order. The correct shape of the structure factor (the function describing the intensity of scattering of X rays or neutrons in the substance) was achieved for a number of particles no less than several thousand.

Lately there has been an upsurge of interest in 'first-principles' molecular dynamics modeling, in which the Schrödinger equation is solved at each step for the current arrangement of the particles. The calculated wave function makes it possible to find the forces acting on the ions of the metal. For simple metals this method was proposed by Car and Parrinello [19]. It was also used for liquid Li, Na, K, and Hg [20], cesium [21], Cu, Ge, V, and Te [22], antimony [23], small clusters of cadmium [24], AuCs alloy [25], liquid NaCl [26], and Ag–Se alloy [27]. These calculations require long computer times even with the use of modern computers and have been carried out only for small systems consisting of several dozen atoms. Theoretical calculations produce results that are in good agreement with the experimental data concerning the shape of the correlation functions.

Methods of constructing atomic models from known pair correlation functions (PCF) form a separate group (a pair correlation function is the probability of finding a pair at a given distance). These are what is known as the inverse Monte Carlo method (IMCM), the methods of Schommers and Reatto, the force and 'hybrid' algorithms, and the method of building a model for a liquid or amorphous alloy using the Born–Green–Bogolyubov equation [28–33]. The main idea underlying all these methods is the construction of a model whose pair correlation function (or partial PCF for alloys) coincides with that obtained for the real object. In all cases the quality of reconstruction of the model from the diffraction data can be estimated by the standard deviation, or discrepancy, between the 'target' and model pair correlation functions and, in the case of two-component systems, from the discrepancies between three partial pair correlation functions (for the pairs 11, 12, and 22). The discrepancies that have been achieved in the best cases are of order 0.005, which means almost complete agreement, while in the worst cases the discrepancy is 0.1 to 0.2 or the process diverges. Here the Reatto and Born–Green–Bogolyubov methods when applied to topologically dense systems of the type of liquid and amorphous metals make it possible to approximately reconstruct pair interparticle potentials, too. For loose systems with small coordination numbers, the process of construction of models of amorphous silica by IMCM is

fraught with difficulties and is possible only for special arrangements of the atoms in the model [34].

The models constructed by IMCM and equivalent methods do not make it possible to study kinetic properties, since the interparticle potentials are unknown. However, in some cases the structural information about the model provides a key for studying diffusion problems. Such, for instance, is the analysis of pores in the structure of loose silica type systems or amorphous semiconductors, which makes it possible to draw conclusions about the presence of easy diffusion paths for particles of moderate size.

3. The cooperative diffusion mechanism. Direct simulation of diffusion in liquid and amorphous phases by the molecular dynamics method

If the interparticle potential is known, calculating the self-diffusion coefficient of a liquid by the molecular dynamics method is fairly easy. In the process of the molecular dynamics of relaxation of a liquid or amorphous phase, the particles of the model at each temporal step (with a step length of about 1 fs) perform small displacements correlated with the displacement of the neighboring particles. Here the cooperative diffusion mechanism is realized. The mean square particle displacement $\langle r^2 \rangle$ is described by the expression

$$\langle r^2 \rangle = a(t) + 6Dt \tag{4}$$

(t is the current time). Initially, the ordinary (Fickian) dependence does not work because of the presence of the contribution $a(t)$ responsible for the vibrational component of motion. However, at large run lengths the term $a(t)$ ceases to change and the time dependence of $\langle r^2 \rangle$ can reach an asymptotic straight line whose slope makes it possible to calculate the self-diffusion coefficient D.

For models of simple liquids, where the self-diffusion coefficients are of order 10^{-5} cm^2 s^{-1}, a run length of several hundred steps is sufficient to obtain good results. For models of viscous liquids (oxide type systems SiO_2, B_2O_3, $CaO-SiO_2$), where the self-diffusion coefficients near the melting point (T_m) are of order 10^{-6} cm^2 s^{-1}, the run lengths must be increased to several ten thousand steps, since for shorter run lengths the time dependence of $\langle r^2 \rangle$ is unable to reach its asymptote. But if the self-diffusion coefficient is of order 10^{-7} cm^2 s^{-1} or smaller, it is practically impossible to determine this coefficient by the molecular dynamics (MD) method at typical operating speeds of ordinary computers.

The MD method makes it possible to easily study the effect of such factors as temperature, pressure, and particle mass on the diffusion coefficients (the isotopic effect). In the simplest case of a hard-spheres liquid, the particle mobility is determined by the dimensionless parameter $D(m/kT)^{1/2}/\sigma$, where m is the particle mass, σ is the particle diameter, T is the temperature, and k is Boltzmann's constant. At a constant temperature, this parameter, calculated by the MD method, linearly decreases with volume, so that the self-diffusion coefficient already cannot be measured for $V/V_0 < 1.45$, where V_0 is the volume of the corresponding closely packed crystal at $T = 0$ [35]. For the maximum packing factor in the disordered hard-spheres model, $\eta = 0.6366$ (when $V/V_0 \cong 1.162$), the extrapolated mobility of the particles (spheres) disappears completely. The diffusion mobility in a liquid with a Lennard-Jones potential behaves in a similar manner [36]. Here the self-diffusion coefficient decreases almost to zero (i.e. becomes smaller than 10^{-6} cm^2 s^{-1}) at $V/V_0 \cong 1.03$ in the case of isothermal compression and at $V/V_0 \cong 1.12$ in the case of cooling under zero pressure.

When models of dense noncrystalline systems with short-range pair potentials (argon and metals) are considered, pressure enhancement usually results in a decrease of the self-diffusion coefficient. Other situations may also emerge, however. For the case of a pair Gauss potential $u(r) = u_0 \exp(-br^2)$, Stillinger and Weber discovered an anomalous increase of the self-diffusion coefficient on compression of the system. This effect emerges because as the distance decreases, the force function $-\mathrm{d}u(r)/\mathrm{d}r$ passes through a maximum and then decreases, too. Another example of anomalous behavior is presented by loose structures of the silica type, where the structure changes under pressure, the coordination numbers grow, and three-body contributions to the potential begin to play a smaller role. For instance, in the MD modeling of silica in the ionic variant at 1400 K, a rise in pressure up to 12 GPa was found to lead to an increase of the ion self-diffusion coefficients severalfold, and under a further increase of pressure up to 36 GPa these coefficients slowly decreased [37]. The enhancement of the ionic mobility in MD models of liquid silica under pressure was also studied by Tsuneyuki and Matsui [38].

If, to describe the temperature dependence of the diffusion coefficient D of simple liquids, we use the Arrhenius equation $D = D_0 \exp(-E/kT)$, where E is the effective activation energy, it occurs that E exponentially grows as the temperature of the system is lowered [36]. Deviations become especially evident in the region of small D's. The reason is that actually the diffusion mechanism in simple liquids is not of an activation nature. An approximate theoretical estimate of the temperature dependence for such a mechanism yields the formula $D = aT^2$ [39], which fairly well describes the data obtained under microgravitation for indium, lead, and antimony [40]. A power-law dependence $D = 4.2 \times 10^{-11} T^{2.3596}$ cm^2 s^{-1} was obtained, in particular, by the MD method for liquid cesium in the 323 – 1923 K range [151].

However, such a dependence does not agree with the experimental data for highly supercooled liquids and it cannot be extrapolated to the low-temperature range. At the glass transition temperature it yields excessively high values for D, of order 10^{-8} cm^2 s^{-1}, while the experimental data are near 10^{-18} or even smaller. The cooperative diffusion mechanism characteristic of liquids becomes 'frozen', and the motion of the particles becomes oscillatory near an almost immobile position of equilibrium determined by the arrangement of the surrounding atoms [36, 41].

Unfortunately, this 'frozen' mechanism has not yet been observed by the MD method, since the method is unable to study such slow diffusion processes by using the existing algorithms. More than that, for a supercooled liquid the MD method often overestimates the self-diffusion coefficients. For instance, in models of systems with a Lennard–Jones potential, an appreciable value of the self-diffusion coefficient (larger than 10^{-7} cm^2 s^{-1}) is obtained at temperature even near $0.1T_m$, where T_m is the melting point. For the ionic models of KCl, Woodcock et al. [42] observed an appreciable self-diffusion coefficient ($D \sim 10^{-6}$ cm^2 s^{-1}) at temperatures of about $0.4T_m$. Examples of the opposite are also known. In the ionic models of SiO_2, self-diffusion can be observed using the MD method only near 2500 K [42], i.e. at much higher temperature than the melting point.

The fact that the molecular-dynamics self-diffusion coefficients at reduced temperatures are overestimated in comparison to the actual values may be due to the small size of the models and their nonequilibrium nature, which is caused by the high rates of computer cooling. Another reason may be the effect of real weak long-range forces, which is either ignored in calculations or cannot be properly taken into account. Pavlov [43] even suggested incorporating special forces stabilizing the crystalline structure in the MD modeling of solidification processes. Possibly, this problem will be solved in the near future within the scope of the classical MD method by using new algorithms and powerful computers, which will make it possible to study systems consisting of at least several million particles.

Under conditions where the cooperative diffusion mechanism is realized, the effects of structure relaxation, which are related to a process in which a strongly nonequilibrium system approaches a more equilibrium state, can be observed in model experiments. If the initial state of the amorphous model is obtained by rapidly cooling the liquid model, then in the process of static relaxation or molecular dynamics annealing one observes a gradual drop in pressure at constant volume or a gradual decrease in volume at constant pressure (depending on the simulation algorithm) [10]. For metal alloys, the decrease in volume amounts to 0.5–1.0% and is close to the observed experimental values. However, in one-component model systems the times of such relaxation are too short (of the order of tens of picoseconds) to correspond to processes in real alloys. In two-component model amorphous systems the diffusion coefficients are much smaller, but the time scale of 'cooperative' relaxation is still too far from the real one.

Various physical models and analytical methods have been suggested for a description of the cooperative diffusion mechanism in supercooled liquids (e.g., see Refs [44, 45]). In particular, it was suggested that atoms should be divided into solid-like, which cannot move, and liquid-like, which participate in the diffusion motion [46]. The effective volume of the cell in which a particle exists and the ratio of this volume to a certain critical volume determine to which class the particle belongs. For instance, in a system with a purely repulsive pair potential of the type $u(r) = \varepsilon(r_0/r)^{12}$, where r is the atomic separation and ε and r_0 are parameters, the decisive role is played by the dimensionless parameter $\rho^* = (Nr_0^3/V)(\varepsilon/kT)^{1/4}$, where N is the number of particles in a volume V. When ρ^* of a noncrystalline grows from 1.1 to 1.5 (via compression or cooling), the fraction of liquid-like particles decreases from 1 to 0, which affects diffusion [46]. This criterion is not of a purely structural nature and reflects the idea of a relation between particle mobility (and viscosity, in the spirit of Bachinskiĭ) and free volume. Using the terminology of statistical mechanics, we can say that liquid-like particles are excited. Akhiezer et al. [47] carried out calculations of self-diffusion coefficients for amorphous metal alloys under the assumption that diffusion takes place when several excited atoms are close to each other. Here local transformation of the structure, which is an elementary act of diffusion, is possible. In the final analysis, such an approach leads to a model in which as the temperature rises, the diffusion coefficient for an amorphous alloy continuously transforms into the diffusion coefficient for the liquid.

In noncrystalline systems, the cooperative mechanism can, at least in principle, accompany by the hopping mechanism. After an activated hop of one of the particles has been completed, the other particles are displaced in the process of relaxation over small distances, which also contributes to the mean square particle displacement. Fam Khak Huang et al. [48, 49] studied this possibility using models of amorphous iron as examples. The sum of the squares of the cooperative displacement of all the atoms in the model under continuous static relaxation, which accompanies the hopping of an atom from a site to a neighboring vacancy, was found to be slightly smaller than the square of the particle hopping length. Thus, the cooperative 'accompaniment' of activated hops increases the contribution from the pure hopping mechanism insignificantly (by a factor of approximately two). For other amorphous systems, the ratio of these contributions may be different, but it is unlikely that the overall picture will be much different.

Thus, in the region of stability of the liquid state the MD method makes it possible to calculate easily and reliably the diffusion coefficients if the interparticle interaction potentials are known. However, recent years have seen no real progress in the analysis of the cooperative diffusion mechanism for the deep supercooling region. It is quite possible that this problem will be solved in the near future as a result of using powerful computers to simulate diffusion in systems consisting of 10^4–10^6 particles with long diffusion times.

4. Activation mechanisms of diffusion

The diffusion 'walk' of a particle in a crystal occurs via transitions of this particle, activated by thermal energy, across potential barriers from one stable (saddle) state to a neighboring stable state. This is known as the hopping mechanism, and the barrier height E_{act} is called the activation energy. This energy usually amounts to tens of kilojoules per mole. The hops take place in different directions. Hence it occurs that the mean square of the particle displacement after n hops, $\langle(\Delta\delta)^2\rangle$ (in units of length of a single hop) is n (here we ignore correlation effects inherent in diffusion in crystals). The temperature dependence of the diffusion coefficient has the form $D = D_0 \exp(-E_{act}/kT)$, where k is Boltzmann's constant. Such temperature dependence as known as the Arrhenius law.

Direct application of the MD method in studies of the hopping mechanism is extremely complicated, not only for the amorphous phase but also for the crystal phase. With a small model we would have to wait a very long time before an activated hop of a particle to a neighboring stable state (a vacant site or an interstice) is realized because the hopping probability $\exp(-E_{act}/kT)$ is usually much smaller than unity and, more than that, thermal activation in a small model is highly improbable. True, studying the liquid silica model, Woodcock et al. [42] found that at 6000 K there are infrequent spontaneous hops of oxygen ions between the coordination spheres of two neighboring silicon ions. This was proof that the hopping (activation) mechanism of self-diffusion in a noncrystalline system is realizable.

And yet it is extremely difficult to observe the hopping self-diffusion mechanism at the temperatures of amorphous states using the MD method. Other methods are required. The most suitable one was found to be the Monte Carlo method. To establish the characteristic features of activation diffusion in disordered systems, it is convenient to use what is known as disordered lattices, in which the ordered arrangement of the sites is retained but the properties of the particles at different sites are different.

4.1 Distributions of the energies of the stable and transition states. The average time between hops of a diffusing particle. The correlation factor. Calculations of the self-diffusion coefficient

Consider a regular system of sites along which a particle can diffuse. In simple crystalline structures, all stable states of atoms and all transition states may be equivalent energywise. The presence of distributions of the energies of stable and transition states in a disordered system even when there is a regular lattice of sites leads to two specific effects [50, 51]. The first consists in the fact that particle prefers to leave a site across lower barriers. Hence the real path of a diffusing particle is enriched with lower barriers compared to the general set of barriers in the entire system. This effect reduces the average time of site occupation by a particle and enhances the diffusion coefficient. However, this also increases the number of return hops of the particle from the new site to the initial site, since the transition state between these sites has a reduced energy (in model calculations this effect was probably observed in 1980 by Kijek et al. [52]). This 'correlation' effect lowers the diffusion coefficient. In this case, instead of the ordinary expression for the mean square of particle displacement after n hops, $\langle(\Delta\delta)^2\rangle = n$, we should write [53]

$$\langle(\Delta\delta)^2\rangle = Fn\,, \tag{5}$$

where F is the correlation factor. The presence of these two effects, specific to diffusion in a disordered system, was also noted by Limoge and Bocquet [54]. Allowing for these ideas, we can write the expression for the self-diffusion coefficient as

$$D = \gamma\,\frac{d^2}{\tau}\,F\,, \tag{6}$$

where γ is the ordinary geometrical factor, d is the mean hop length, and τ is the average time between hops. In the case of a crystal, $F = 1$ and $\tau = \tau_0\exp(E_{\rm act}/kT)$, where τ_0 is the period of atomic vibrations at a lattice site. The situation with disordered systems is considered below.

Note that the term 'correlation factor' carries different meanings in the literature in relation to different physical phenomena [55, 56].

Akhiezer and Davydov [57] discussed the analytic limit of very low temperatures and broad distributions of the activation-barrier heights. In this limit the time of motion of a particle along its path is equal to the time necessary to surmount the highest barrier in its path. The researchers reduced the diffusion problem to a percolation problem and found that the pre-exponential factor D_0 is much smaller than in a crystal. More than that, according to Akhiezer and Davydov [57], over small times, where the diffusion path is small (several atomic separations), the ordinary Fick diffusion law (4) breaks down. As we will see, there is no way in which such a diffusion mode can be realized in numerical experiments.

Suppose that in a disordered system the energies of the stable states, ε_i, and of the transition states, ε_{ij}, i.e. between sites i and j, are not fixed and are described by the respective distributions. A particle at a given site has the possibility of hopping through any neighboring transition state.

Let us find the average time that the particle stays at a given site. For a hop over the sth barrier this time is, on the average,

$$\tau_s = \tau_0\exp\left(\frac{E_s}{kT}\right), \tag{7}$$

where E_s is the height of the sth barrier, and τ_0 is the period of vibrations of the atom at the site. Since the atom can choose between z directions of the hop, the conditional probability f_n of surmounting precisely the nth barrier is

$$f_n = \frac{\exp(-E_n/kT)}{\sum_{s=1}^{z}\exp(-E_s/kT)}\,. \tag{8}$$

Whence the average time that the particle stays at the given site is

$$\tau_{\rm av} = \sum_{n=1}^{z}\tau_n f_n = \frac{z\tau_0}{\sum_{s=1}^{z}\exp(-E_s/kT)}\,. \tag{9}$$

Since the height of the barrier is $E_s = \varepsilon_{ij} - \varepsilon_i$ (i is the number of the site, and ij represents the transition state between the neighboring ith and jth sites), formula (9) can be written as [50]

$$\tau_{{\rm av}\,i} = \frac{z\tau_0\exp(-\varepsilon_i)}{\sum_{j=1}^{z}\exp(-\varepsilon_{ij}/kT)}\,. \tag{10}$$

This time is different for each site. The importance of the spectrum of lifetimes of particles at sites has been repeatedly stressed by researchers. To calculate the diffusion coefficient one must know the average lifetime $\tau_{\rm av}$ for the entire system of sites. However, simply averaging over the sites will not do since the attendance differs from site to site. Actually, this time depends on the size of the region visited by the particle in the course of diffusion. In Ref. [51], the calculation of $\tau_{\rm av}$ is done under the assumption that a particle wanders from site to site for a long time and visits each site many times. Then the time that it stays at the ith site is proportional to the Boltzmann factor $\exp(-\varepsilon_i/kT)$. The 'equilibrium' average time between hops calculated by this method is

$$\tau_{\rm eq} = z\tau_0\,\frac{\sum_{i=1}^{N}\exp(-\varepsilon_i/kT)}{\sum_{i=1}^{N}\sum_{j=1}^{z}\exp(-\varepsilon_{ij}/kT)}\,. \tag{11}$$

Here each transition state is included twice in the sum. The larger the volume through which a particle passes in the course of diffusion, the more precise formula (11) is, since over short diffusion paths the specific distribution of the energies of the stable and transition states may differ from the average distribution.

Formula (11) can be used for specific distributions of the energies of the stable and transition states. For instance, for normal distributions cut off at the deviations $\pm 2\sigma$, Ref. [51] yields

$$\frac{\tau_{\rm eq}}{\tau^*} = \exp\left[\frac{\sigma_{\rm s}^2 - \sigma_{\rm b}^2}{2(kT)^2}\right]\frac{\xi_{\rm s}}{\xi_{\rm b}}\,. \tag{12}$$

Here $\sigma_{\rm s}$ and $\sigma_{\rm b}$ are the standard deviations of the energies of the stable and transition states, and τ^* is the lifetime of a particle at a site in the case of an ordered system, where the energies of the stable and transition states are equal to the corresponding average values for a disordered system. We shall call such a system *dual* in relation to our disordered

system. The quantities ξ_s are given by the formula

$$\xi_s = \operatorname{erf}\left(\frac{\sigma_s}{\sqrt{2}kT} + \sqrt{2}\right) - \operatorname{erf}\left(\frac{\sigma_s}{\sqrt{2}kT} - \sqrt{2}\right). \qquad (13)$$

Here the subscript 's' stands for the stable state (s) or for the barrier (transition) state (b). Similar expressions for ξ_s have also been obtained for cut-off uniform and rectangular distributions [51]. From Eqn (13) we see that an increase in the width of the distributions of the stable states increases the average time between hops, while an increase in the width of the distributions of the transition states reduces the average time between hops. A similar formula for the average time was obtained by Gorbunov and Klinger [58]. For close values of the variances of these two distributions, the average time may prove to be equal to the average time in a dual ordered system [51, 54].

We will now discuss the correlation factor. An estimate of this factor can be found in Ref. [50]. A diffusing particle prefers the lowest barrier when it leaves its site. At low temperatures this happens practically always. In Ref. [50], the concept of a $1N$-dead end was introduced as a site that a particle (or vacancy) leaves after N repeated hops across the same barrier. The probability that a given ith site is a $1N$-dead end is

$$f_N = \frac{\sum_{s=1}^{z} \exp(-NE_s/kT)}{\left[\sum_{s=1}^{z} \exp(-E_s/kT)\right]^N}. \qquad (14)$$

Two adjacent dead ends are called a trap if a particle performs recurring hops from one dead end to the other and back. The correlation factor determines the intensity of trapping a diffusing particle by traps and is related directly to the probability f_N from Eqn (14). If we take $E_s = \varepsilon_{ij} - \varepsilon_i$, Eqn (14) immediately shows that f_N and hence the correlation factor F are entirely independent of the distribution of the stable states ε_i. The results for F were obtained in Ref. [50] by various approximation schemes. More precise values of the correlation factor can be found by direct computer simulation of self-diffusion in disordered systems.

According to Ref. [50], activated diffusion in a disordered system proceeds as follows. An atom performs random walks and surmounts activation barriers of various heights in the process. Sometimes it meets a trap and performs a certain number of hops within it, after which it leaves the trap and migrates to the next trap. To find the self-diffusion coefficient we must determine the average number of hops that an atom does as it travels from one trap to another and the average number of hops inside a trap. The average number of hops that a particle performs in its travel from one trap to another depends on $\bar{f}_2$. In Ref. [50], an analytic expression was derived for the average number of hops of a particle traveling from one trap to another:

$$v = \left[1 - (1 - \bar{f}_2^2)^{1-1/z}\right]^{-1},$$

where z is the coordination number. For $z = 10$ we have the values of the number of hops:

$\bar{f}_2$	0.1	0.3	0.5	0.7	0.8	0.9	1
v	111	12.3	4.4	2.2	1.7	1.3	1

At high temperatures ($kT \gg E_s$), all the barriers are of equal height, and $\bar{f}_2 = 1/z = 0.1$ and $v = 111$. At low temperatures the probabilities $\bar{f}_2$ are close to unity and $v \to 1$. This means that a particle meets a trap immediately after it leaves the previous trap.

The average number of hops that a particle does inside a trap was also calculated in Ref. [50]. As a result, the correlation factor is given by the formula

$$F = \left[1 + \frac{1}{v}\left(2.5 + 2\sum_{N=2}^{\infty}\frac{\bar{f}_N^2}{\bar{f}_2^2}\right)\right]^{-1}, \qquad (15)$$

where v is the average number of particle hops between two traps. Approximate analytic calculations of the correlation factor for the case of a triangular distribution of barrier heights were also done in Ref. [50]. It was found that $\bar{f}_2 \cong 0.10 + 0.90\exp(-6.02kT/\Delta\varepsilon)$, where $\Delta\varepsilon$ is the halfwidth of the barrier-height distribution. At low temperatures a particle is so firmly trapped that the correlation factor is practically nil [50]. More precise values of the correlation factor can be found by direct computer simulation of self-diffusion in disordered systems.

In Ref. [59], analytic calculations were done for different barrier-height distributions: a normal distribution, a triangular distribution, etc. If the set of barriers at a given site is chosen at random, the effective self-diffusion activation energy usually increases with decreasing temperature. For sets of barriers at a given site that are chosen not at random, the effective activation energy may decrease with temperature. The wider the barrier-height distribution, the smaller the correlation factor. It was found that the pre-exponential factor D_0 may be either larger or smaller than the ordinary value.

Limoge and Bocquet [54] found, by analytic means, an approximate expression for self-diffusion in a disordered system:

$$\frac{D}{D^*} = \exp\left[\frac{f\sigma_b^2 - \sigma_s^2}{2(kT)^2}\right]. \qquad (16)$$

Here D^* is the coefficient of self-diffusion in a dual ordered system. The correlation factor is present in Eqn (16) implicitly in the form of the coefficient $f < 1$, thus reducing the diffusion mobility. In our notation, the factor F and the coefficient f are connected by the relation $F = \exp\left[(f-1)\sigma_b^2/2(kT)^2\right]$. The values of f were calculated by Limoge and Bocquet [54] by the Monte Carlo method, and at $\sigma_b/kT = 3.6$ amount to 0.15 to 0.64 for different lattices. This leads to values of F ranging from 0.004 to 0.1, and they decrease as the coordination number decreases from 12 to 4. As a result, the researchers found that temperature dependence of the self-diffusion coefficient is of Arrhenius type even as D changes over eight orders of magnitude. However, in the general case, temperature dependence is clearly non-Arrhenius.

4.2 Computer simulation of activated self-diffusion

In this section we will discuss the diffusion processes in what is known as disordered lattices, i.e. systems that possess long-range order in the arrangement of sites but are disordered in relation to the energies of the stable and transition states.

4.2.1 Computer simulation of diffusion in a one-dimensional disordered system. Linear models are widely used in solid-state physics to study the mechanisms of various processes and calculate the characteristics of the processes. The diffusion process can be examined using the example of an

ordered linear chain of sites (Albert Einstein). One example of a real object described by such a model is a dislocation tube, where the periodic field is perturbed by various atoms adsorbed on a dislocation at random.

The mathematical aspects of the problem of random walks of a particle along an infinite linear chain of sites with a given distribution of the probability of transition to right and left have been considered by many researchers (see the review of Haus and Kehr [56]). In view of the fact that for an infinitely long chain of sites there is a finite probability of a particle meeting any number of successive potential barriers, the ordinary diffusion law (5) may break down. Sinai [60] arrived at an asymptotic result for the mean particle displacement: $|\Delta r| \sim \ln^2 n$. The same result for some types of distributions of the probability of a particle leaving a site was obtained by Obukhov [61] for a planar system. However, an exact analytic solution for a regular system of sites with the same stable states [56, 62] but different transition states lead to the ordinary diffusion law (5) in the limit of long diffusion times. When there is a distribution of energies of the stable states with equal transition states, the diffusion law works for all times [56, 63]. The analysis of two- and three-dimensional disordered systems also leads to the ordinary diffusion law (5) [56].

Sinai [60] specified the probabilities of a particle moving to the left and right of a given site in the form of random quantities and excluded all correlations between these probabilities at different sites. However, in real thermally activated diffusion, there must be a slight correlation between these probabilities, since for each pair of neighboring states there is a unique transition state. Note that the transition probability is determined by Boltzmann statistics. More than that, real objects cannot be infinitely long, and the diffusion time is finite.

Generally speaking, in a disordered system there may be a difference between the diffusion coefficients measured in stationary and nonstationary experiments. In the first case the average occupancy of the sites is time-independent, while in the second it varies with time. In other words, in the stationary case all deep energy states are already occupied, while in the nonstationary case they gradually become saturated by the diffusing particles. The results of computer calculations of steady-state diffusion of an impurity along a linear chain of sites can be found in Ref. [64]. If the concentrations C_1 and C_N at the ends of the chain are fixed, after sufficient time has passed the system will find itself in a steady state with a constant flux of particles along the entire chain. The condition for constancy of flux makes it possible to calculate the concentration at all sites and find the coefficient D of steady-state diffusion along the chain. Analysis shows that the ratio D/D^*, where D^* is the diffusion coefficient in the dual system, is independent of the energies of the stable states:

$$\frac{D_{\rm st}}{D^*} = \frac{N-1}{\sum_{i=1}^{N-1} \exp(\Delta\varepsilon_{ij}/kT)} \tag{17}$$

with $\Delta\varepsilon_{ij} = \varepsilon_{ij} - \langle\varepsilon_{ij}\rangle$. For the average time between particle hops we have the expression (τ^* is the value of this time for the dual system, in which all $\Delta\varepsilon_{i,\,i+1} = 0$)

$$\frac{\tau_{\rm st}}{\tau^*} = \frac{2(N-1)}{\sum_{i=1}^{N-1}\sum_{j=1}^{z} \exp(-\Delta\varepsilon_{ij}/kT)} \,. \tag{18}$$

The sum with respect to j in the denominator is over all transition states (the coordination number $z = 2$). The correlation factor is described by the equation

$$F = \frac{(N-1)^2}{\sum_1^{N-1} \exp(-\Delta\varepsilon_{ij}/kT) \sum_1^{N-1} \exp(\Delta\varepsilon_{ij}/kT)} \,. \tag{19}$$

The sums in the denominators are also over all transition states. As expected, the factor F is independent of the distribution of the energies of the stable states.

In the case of non-steady-state diffusion along the chain, the average time $\tau_{\rm st}$ must be replaced by the 'equilibrium' time $\tau_{\rm eq}$, which is given by Eqn (11) or the equivalent expression [51]

$$\frac{\tau_{\rm eq}}{\tau^*} = z\, \frac{\sum_1^{N-1} \exp(-\Delta\varepsilon_i/kT)}{\sum_1^{N-1}\sum_{j=1}^{z} \exp(-\Delta\varepsilon_{ij}/kT)} \,. \tag{20}$$

Allowing for the fact that $D_{\rm st}/D^* = F\tau^*/\tau_{\rm st}$, we arrive at a formula for non-steady-state diffusion along the chain:

$$\frac{D}{D^*} = \frac{(N-1)^2}{\sum_1^{N-1} \exp(-\Delta\varepsilon_i/kT) \sum_1^{N-1} \exp(\Delta\varepsilon_{ij}/kT)} \,. \tag{21}$$

Expressions similar to Eqns (20) and (21) were also found by Gorbunov and Klinger [58], who used a different method. By comparing Eqns (17) and (21) we see that the non-steady and steady-state diffusion coefficients coincide only if the energies of all stable states are the same. The same is true of the ratio τ/τ^*.

In Ref. [64], a chain of sites was examined in which all the energies ε_i are the same and the energies of the transition states take only two values $\varepsilon_{\rm b1}$ and $\varepsilon_{\rm b2}$ (a dichotomous system). The concentration of the low transition states (with energy $\varepsilon_{\rm b1}$) is α_1 and that of the other transition states, $\alpha_2 = 1 - \alpha_1$. We introduce the notation $\Delta\varepsilon = \varepsilon_{\rm b2} - \varepsilon_{\rm b1}$. Then

$$F = \frac{1}{1 + 2\alpha_1\alpha_2 \left[\cosh(\Delta\varepsilon/kT) - 1\right]} \,, \tag{22}$$

$$\frac{\tau_{\rm st}}{\tau^*} = \frac{1}{\alpha_1 \exp(\alpha_2\Delta\varepsilon/kT) + \alpha_2 \exp(-\alpha_1\Delta\varepsilon/kT)} \,, \tag{23}$$

$$\frac{D_{\rm st}}{D^*} = \frac{\exp(\alpha_2\Delta\varepsilon/kT)}{\alpha_1 + \alpha_2 \exp(\Delta\varepsilon/kT)} \,. \tag{24}$$

Direct computer simulation of diffusion along a chain of sites has shown that Eqns (23) and (24) are true to within an error of 3–6%. Good agreement has been achieved for the correlation factor. This agreement worsens somewhat as the temperature is lowered because the particle does many recurring hops and does not travel far from its initial position. Here the specific set of heights of the barriers being surmounted does not represent the entire distribution.

In Ref. [64] it was found that at $\sigma_{\rm s}/kT = 1.58$ (for stable states) the steady-state diffusion coefficient exceeds the non-steady-state coefficient by a factor of four. The discrepancy between these two quantities must grow as the temperature is lowered. There is no such discrepancy in systems with $\sigma_{\rm s} = 0$.

This effect should be observed in real three-dimensional systems. The reason for the effect lies in the process of buildup of the diffusing component in non-steady-state diffusion at sites with a reduced energy ε_i, a process resembling the case of diffusion with internal adsorption. On the other hand, in a steady state the concentrations are time-independent and the

spread of the energies ε_i does not manifest itself. By comparing the diffusion coefficients in the nonstationary and stationary process we would be able, at least in principle, to determine the width of the saddle-state energy distribution for the particle belonging to the diffusing component.

When examining impurity diffusion in an amorphous metal, one should allow for the relaxation of the solvent atoms surrounding an impurity, since as a result of such relaxation the energies of the stable and transition states after the atom has hopped may differ from the energies of these states before the hop. In this case the initial values of the energies become forgotten partially or completely. Fam Khak Huang et al. [65] studied the role of this effect in diffusion using a linear system as an example. The length of the linear segment under investigation amounted to one thousand sites. Initially the particle was placed at the 500th site. Diffusion was calculated by the probability-field method (by solving what is known as the master equation) [51]. The probability field has the form

$$P_i(n+1) = P_{i-l}(n)q_{i-l,\,i} + P_{i+l}(n)q_{i+l,\,i}\,. \tag{25}$$

Here n is the number of the step, and i is the number of the site, $P_i(n)$ is the probability of finding the diffusing particle at the ith site after the nth step has been completed, and $q_{i,\,l}$ is the relative probability of the particle hopping from the ith level to the neighboring lth level. If the initial probability distribution $P_i(0)$ is known, we can use Eqn (25) to calculate $P_i(n)$ at each step and thus study the diffusion process. This equation can be used in systems with any number of dimensions.

The initial sets of energies of the stable and transition states for each atom can change with the passage of time. It was found that as the degree of 'forgetfulness' of the initial energy values ε_{b0} increases, the correlation factor tends to unity and the average time between particle hops, to the 'equilibrium' time calculated using Eqn (11).

As is known, the velocity W of the drift initiated by an external field g is determined by the Einstein equation

$$W = \frac{Dg}{kT}\,. \tag{26}$$

Fam Khak Huang et al. [66, 67] checked the validity of this equation for disordered systems. To this end the researchers studied diffusion in a linear and a three-dimensional disordered lattices by the probability-field method [51] and by measuring the variation in the drift velocity in the presence of a constant external force. The energy distributions for the stable and transition states had the shape of normal distributions cut off at 2σ. Einstein's equation was found to be valid within 5–10% for all cases that were investigated.

4.2.2 Computer simulation of diffusion in a two-dimensional disordered system. A description of the mathematical methods used in solving the diffusion problem for two-dimensional disordered lattices can be found in the review by Haus and Kehr [56]. For long times we have the diffusion law (5). In Ref. [68], the relationship that exists between the coefficients of self-diffusion of vacancies (D_v) and of atoms (D_a) in a disordered square lattice was examined. A square grid with 100×100 sites and with periodic boundary conditions was taken. The energies of the stable states at each site were set equal. The distribution of the transition states was assumed to be either uniform over a segment or normal. One of the atoms was removed from the grid, which resulted in the formation of a vacancy occupying the previous position of the atom. Then the vacancy was interchanged many times with the neighboring atoms. The coefficients D_v and D_a were found by calculating the mean squares of the displacements of the atoms or the vacancy. The results of these calculations are listed in Table 1, where F_a and F_v stand for the correlation factors for atoms and vacancies, τ_{real} is the real average time between two hops, σ_b^2 the real variance of the distribution of the energies of the transition (barrier) states, and τ^* and D^* are the parameters of the dual ordered system.

The data listed in Table 1 show that the vacancy correlation factor F_v and the coefficient D_v are always larger than F_a and D_a, respectively. In disordered systems, the ratio f of the self-diffusion coefficients for the vacancy and the atoms are weakly temperature-dependent and are close to the value of f for an ordered system (where $\sigma_b = 0$).

4.2.3 Computer simulation of diffusion in a three-dimensional disordered system. A description of the mathematical methods used in solving the diffusion problem for three-dimensional disordered lattices can be found in the review by Haus and Kehr [56]. Here the diffusion law (5) is also asymptotically valid, and this is corroborated by simulations that use the Monte Carlo method. The results of computer simulations of self-diffusion in a double-barrier (dichotomous) system can be found in Ref. [53]. The system consisted of a simple cubic lattice containing $11 \times 11 \times 21$ sites, and the particles were forbidden to reach the lateral faces of the cube. The energies of the stable states were the same, and the energies of the transition states took only two values, ε_1 and ε_2 (the fraction of the first type of states was α_1). The

Table 1. Diffusion in a two-dimensional disordered system.

Type of distribution	σ_b/kT	τ_{real}/τ^*	For vacancies		For atoms		$f = D_a/X_vD_v$
			F_v	D_v/D_v^*	F_a	D_a/D_a^*	
Normal	0	1	1	1	0.469	1	0.469
	0.880	0.684	0.693	1.013	0.316	0.981	0.455
	1.759	0.255	0.258	1.014	0.120	1.004	0.465
	2.640	0.065	0.078	1.213	0.038	1.268	0.490
	3.518	0.013	0.024	1.785	0.012	2.002	0.527
Uniform	0	1	1	1	0.469	1	0.469
	1.443	0.500	0.558	1.110	0.263	1.121	0.471
	2.309	0.147	0.167	1.130	0.079	1.138	0.471
	3.464	0.029	0.051	1.750	0.027	1.993	0.534
	4.330	0.008	0.024	3.037	0.014	3.833	0.592

Table 2. Diffusion in a three-dimensional double-barrier disordered system.

$\Delta\varepsilon/kT$	α_1	F	F by (15)	$\tau_{\text{real}}/\tau_1$	τ_{eq}/τ_1	D/D_1	D/D^*
3	0	1	1	20.1	20.1	0.05	1
	0.10	0.444	0.596	7.50	6.91	0.059	0.88
	0.40	0.545	0.601	2.54	2.33	0.214	1.29
	0.80	0.910	0.853	1.36	1.23	0.668	1.22
5	0.05	0.139	0.377	21.4	17.7	0.0065	0.75
	0.10	0.079	0.216	10.0	9.43	0.0079	0.71
	0.2	0.079	0.173	4.94	4.87	0.016	0.87
	0.40	0.259	0.366	2.83	2.47	0.092	1.85
	0.8	0.873	0.873	1.37	1.25	0.0638	1.73
7	0.05	0.022	0.088	20.0	19.7	0.0011	0.85
	0.10	0.013	0.040	11.7	9.92	0.0011	0.60
	0.20	0.012	0.032	5.00	4.98	0.0024	0.65
	0.40	0.178	0.119	2.96	2.50	0.060	4.00
	0.80	0.867	0.842	1.37	1.25	0.633	2.57

calculations were done by the probability-field method, and a run consisted of 2000 to 4000 hops of a particle.

The calculated quantity was the total probability $w(n)$ of a particle occupying the half of the parallelepiped farthest from the face where the particle had been initially (i.e. the last ten layers). Then the same calculation was done for the dual system, in which all the energies of the transition states are equal to the average energy for the disordered system. If for the same probability $w(n)$ the number of hops in the ordered and disordered systems is n_0 and n_1, respectively, the correlation factor is n_0/n_1. The average time between hops was found from Eqns (11) or (20) and by computer simulations, provided that the number of visits by a particle to each site and the average time the particle spends at a given site are known [Eqn (9)].

Table 2 lists the results of calculations for three values of $\Delta\varepsilon/kT = (\varepsilon_2 - \varepsilon_1)/kT$ and different concentrations α_1. We denote the quantities for the ordered system by τ_1 and D_1, in which all energies of the transition states are ε_1.

Table 2 shows that the average time that a particle stays at a site, the real value and the equilibrium value, are very close. More than that, as the temperature becomes lower, the effect of particle trapping becomes stronger. The correlation factor passes through its minimum at $\alpha_1 = 0.2$, where it is much smaller than unity (Fig. 1). The results produced by formula (15) agree satisfactorily with the experimental data, with the formula underestimating them no more than by 10%. The reason for this discrepancy is that the theoretical estimates made in Ref. [50] are based only on the allowance for two-site traps. The fact the multisite traps are ignored leads to overestimation of the factor F near its minimum (in α_1) by approximately 30%, and at $\Delta\varepsilon/kT = 7$ the overestimation is roughly by a factor of 2.5. Thus, even when there are only two different barriers heights, the diffusing particles are effectively trapped.

Figure 2 depicts the dependence of the ratio D/D_1 on the fraction of the lower transition states, α_1, at different temperatures. We see that D/D_1 monotonically decreases as the low-barrier fraction gets smaller.

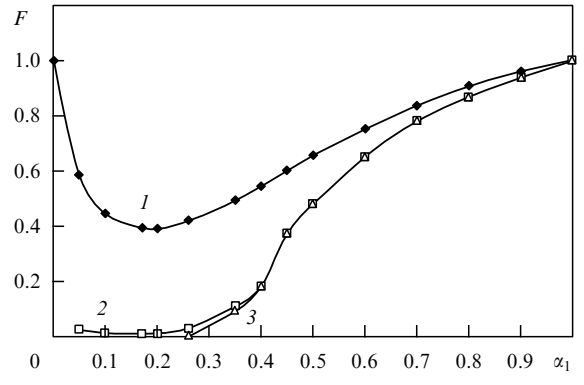

Figure 1. Correlation factor F of a three-dimensional disordered system with a dichotomous distribution of energies of the transition states. All energies of the stable states are the same. The lattice contains $11 \times 11 \times 21$ sites, and diffusion is along the longer edge. The particles are forbidden to reach the lateral faces of the cube. Curve *1* corresponds to $\Delta\varepsilon/kT = 3$, curve *2* to $\Delta\varepsilon/kT = 7$, and curve *3* to $\Delta\varepsilon/kT \to \infty$; α_1 is the fraction of the low transition states [53].

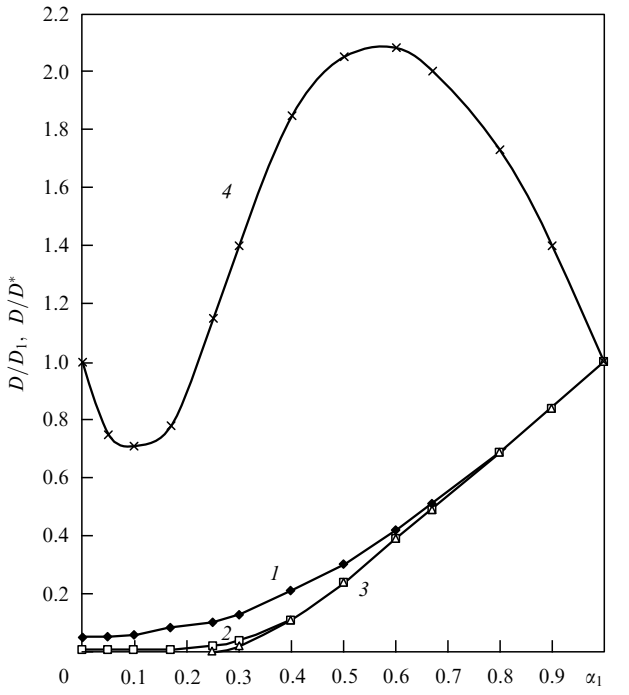

Figure 2. Dependence of the ratios D/D_1 (curves *1–3*) and D/D^* (curve *4*) on the fraction of the low transition states, α_1: D_1 is the diffusion coefficient for the case where all transition states have the energy ε_1, and D^* is the diffusion coefficient for a dual ordered system. The four curves correspond to the following values of $\Delta\varepsilon/kT$: curve *1*, $\Delta\varepsilon/kT = 3$; curve *2*, $\Delta\varepsilon/kT = 5$; curve *3*, $\Delta\varepsilon/kT \to \infty$; and curve *4*, $\Delta\varepsilon/kT = 5$ [53].

Interesting behavior is exhibited by the ratio D/D^*, where D^* is the diffusion coefficient for a dual system (see Table 2 and Fig. 2): it may differ substantially from unity. This means that the effects of reduction of the average lifetime of a particle at a site, and of reduction of the correlation factor as an ordered system is replaced by a disordered one, balance each other only partially, and their 'decompensation' increases as the temperature gets lower.

Introduction of correlations into the arrangement of the low and high transition states has shown that correlations have practically no effect on the average time between the hops of a particle but enhance the correlation factor substantially, especially near the minimum F at a given temperature. This effect is explained by the fact that the buildup of low barriers at certain sites reduces the number of dead ends and, correspondingly, of two-site traps. As a result, the factor F may increase by 15–30%.

In Ref. [51], direct simulation of diffusion was done using models of a simple cubic lattice ($11 \times 11 \times 20$ sites) for three types of distributions of ε_i and ε_{ij}: (A) a normal distribution cut off at $|\Delta\varepsilon| = 2\sigma$, (B) a triangular distribution cut off at $\pm\varepsilon_l$, and (C) a uniform distribution cut off at $\pm\varepsilon_l$. All particles that reached the lateral faces were reflected back into the crystal. The initial distribution of the particles was assumed to be triangular at the left end face of the parallelepiped. What was calculated in the simulation process was the probability $P_i(n)$ of finding the diffusing particle after n steps at the ith site. In the process of diffusion the probability field of finding the particle moved inside the parallelepiped along its long axis. Summing the probabilities $P_i(n)$ over n makes it possible to find the number of hops that the particle has done into the ith site in the diffusion time. Knowing this sum, we can calculate the average real time τ_{real} that the particle stayed at a site and the correlation factor.

The results of these calculations show that the average time between hops indeed depends on the number of hops, i.e. on the diffusion time. For instance, for the distribution A with $\sigma_s/kT = 0$ and $\sigma_b/kT = 3.518$ the following data were obtained:

Number of hops	100	1000	2000	4000	6000
τ/τ^*	0.034	0.020	0.018	0.017	0.017

The quantity with an asterisk refers to the dual crystal. The obtained dependence is due to the nonequilibrium nature of the initial distribution of the concentration in the sample and the fact that the real distribution of the energies of the transition states approaches the given distribution over the entire volume of the lattice (because of expansion of this region). This effect may be the reason why in real systems the diffusion coefficient is time-dependent. However, no significant discrepancies between diffusion over short and long times, which were detected by Akhiezer and Davydov [57], were discovered in this simulation.

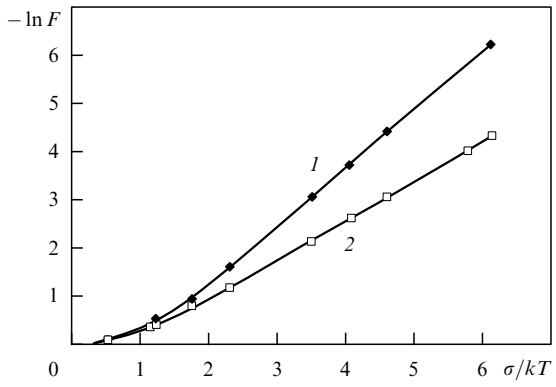

Figure 3. Temperature dependence of the correlation factor: σ is the standard deviation of the energies of the transition states, curve *1* corresponds to the normal and triangular distributions (A and B in Table 3), and curve *2* corresponds to the uniform distribution (C in Table 3) [51].

Several results obtained for the case where $z = 6$ are listed in Table 3. As expected, the average real time τ_{real} that a particle stays at a site is shorter than the average over the sites (the diffusion path follows the lower barriers), with the difference increasing as the temperature is lowered. However, the times τ_{real} and τ_{eq} are close even at the lowest temperatures studied. In accordance with Eqn (11), $\tau_{\text{real}}/\tau^* < 1$ at $\sigma_s/kT = 0$ and $\tau_{\text{real}}/\tau^* > 1$ at $\sigma_b/kT = 0$.

Table 3 shows that the correlation factor strongly depends on the shape of the distribution of ε_b. Figure 3 depicts the dependence of $-\ln F$ on σ_b/kT. In all cases the curves are linear at low temperatures. The following interpolation formulas were proposed in Ref. [51]:

$$-\ln F = a\,\frac{\sigma_b}{kT}\left[1 - \exp\left(-b\,\frac{\sigma_b}{kT}\right)\right], \qquad (27)$$

Table 3. Diffusion in a three-dimensional disordered system.

Type of distribution	σ_b/kT	σ_s/kT	F	τ/τ^*			D/D^*
				Real	Equilibrium by (11)	Averaged over sites	
A	0	0.88	1	1.54	1.37	1.37	0.65
	0.528	0	0.92	0.97	0.88	0.90	0.96
	3.518	0	0.048	0.017	0.014	0.317	2.84
	6.157	0	0.0020	3.0×10^{-4}	6.7×10^{-5}	0.87	6.82
B	1.225	0	0.59	0.54	0.48	0.66	1.10
	4.082	0	0.020	5.8×10^{-3}	4.6×10^{-3}	0.317	3.46
C	1.155	0	0.70	0.60	0.55	0.69	1.16
	2.309	0	0.32	0.16	0.15	0.39	2.16
	4.619	0	0.048	6.7×10^{-3}	5.4×10^{-3}	0.45	7.25
	5.774	0	0.019	1.2×10^{-3}	9.2×10^{-4}	0.45	15.4

where the parameters a and b take the values

Model	A	B	C
a	1.08	1.08	0.79
b	0.44	0.44	0.46

As a result, self-diffusion in a disordered system at $\sigma_s/kT = 0$ proceeds faster than in a dual ordered system. The excess of the coefficient D above D^* was also observed for a double-barrier system (see Fig. 2). This is due to the possibility of the particle choosing the lower barriers in the course of diffusion. But if $\sigma_b/kT = 0$ and $\sigma_s/kT \neq 0$, diffusion proceeds slower than in the respective crystal because of the capture of the diffusing particles by deep stable states. An increase in the width of the distribution of the energies of the transition states lowers the effective activation energy needed for a particle to migrate, and for almost all distributions reduces the pre-exponential factor D_0. An increase in the width of the distribution of the energies of the stable states has the opposite effect.

Thus, the data show that a decrease in the correlation factor and the average time between hops as a result of a crossover from a crystal to a disordered system do not balance each other perfectly, so that the value of the diffusion coefficient for a disordered system may exceed that for a dual system many times over. Hence in theoretical estimates of the diffusion coefficient it is advisable to study the average lifetime and the correlation factor separately.

Diffusion in a three-dimensional system of sites can also be studied by the stationary method. This problem is equivalent to the problem of the conductance of a random grid of resistors connecting neighboring sites. Here the quantity $\Delta\varepsilon/kT$ corresponds to the ratio of resistances of the poor and good conductor, R_2/R_1. Figure 4 depicts the data gathered by calculating the conductance of a grid of resistors on a simple cubic lattice containing $24 \times 24 \times 24$ sites [69] for the cases where $R_2/R_1 = 10$ and ∞. In the diffusion problem these two values correspond to $\Delta\varepsilon/kT = 2.3026$ and ∞. As $\Delta\varepsilon/kT \to \infty$ in the region where $\alpha_1 < 0.25$ (i.e. below the percolation threshold), the diffusion coefficient vanishes because of loss of connectedness in the system of sites, which are connected by low transition states.

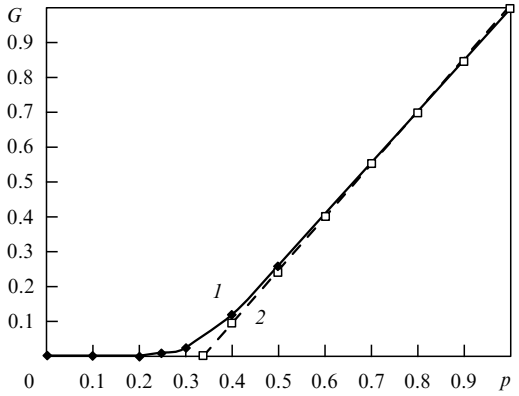

Figure 4. Dependence of the relative conductance G of a grid of resistors on the fraction (p) of randomly positioned resistors with lower resistance for the ratios $R_2/R_1 = 10$ (curve *1*) and ∞ (curve *2*). The lattice is a simple cubic lattice consisting of $24 \times 24 \times 24$ sites with periodic boundary conditions at the lateral faces [69].

The difference between the diffusion coefficients for steady-state and non-steady-state diffusion in a three-dimensional system was studied in Ref. [70] on models of a simple cubic lattice consisting of $11 \times 11 \times 20$ or $9 \times 9 \times 18$ sites (in the latter case, with periodic boundary conditions). In the course of several thousand steps, the mean square of the displacement of a particle is proportional to the number of hops, so that the ordinary diffusion law (4) holds. For steady-state diffusion, the concentrations at the lateral faces of the parallelepiped were fixed. It was found that at $\sigma_s = 0$ the steady-state and non-steady-state diffusion coefficient coincide within experimental error. But if $\sigma_b = 0$ and $\sigma_s \neq 0$, only the non-steady-state diffusion coefficient D changed in relation to D^*; the steady-state diffusion coefficient was found to be insensitive to the distribution of the stable states, as it is in the case of a linear system (see above). Variations in the specific site distribution of the energies have an effect on D that amounts to several percent (for $\sigma_b/kT < 1.76$). The reasons why the steady-state diffusion coefficient differs from the non-steady-state are the same as in the case of a linear system: the initial nonequilibrium of the state and the trapping of the diffusing particle by deeper stable states in non-steady-state diffusion.

Limoge and Bocquet [54] used the Monte Carlo method to simulate the self-diffusion of impurity (tracer) particles in random materials, e.g. amorphous solids. Their data show that for equal energies of transition states the correlation factor is indeed equal to unity and that the distribution of the energies of the transitions states reduces the correlation factor. The resulting activation energy of self diffusion is somewhat lower than the initial activation energy for the ordered crystal.

The same researchers [71] studied random walks along the sites of a three-dimensional disordered system using a Monte Carlo simulation. Here they also found that the effect of disorder in sites and transition states is not additive.

Interesting objects in which the hopping mechanism of self-diffusion can be observed by the MD method are what is known as superionic conductors, such as AgI, Ag_2S, Ag_2Se, Ag_2Te, CaF_2, and $SrCl_2$, in which a transition into the quasiliquid state of one of the ionic sublattices can be observed (the cation sublattice in the case of silver salts and the anion sublattice in CaF_2 and $SrCl_2$) at temperatures below the melting point of the compound [72–75]. Gillan and Dixon [74] constructed MD models of $SrCl_2$ consisting of 324 ions by employing the Born–Mayer–Huggins inter-particle potentials [13]. The time dependence of the mean square displacement of anions had the shape characteristic of liquids (a section of initial rise that transforms into an approximately linear dependence). The anion self-diffusion coefficient in the model increased rapidly in the interval between 1200 and 1300 K to values of order 10^{-5} cm^2 s^{-1} characteristic of liquids, although the cation sublattice remained rigid. However, here the diffusion mechanism proved to be of the hopping type, and in the diffusion events the anions used the octahedral pores of the fluorite lattice. The time between anion hops is approximately one-tenth of the time that an anion stays at a site. It was also found possible to identify the diffusion events along vacancies and interstices, and the concentration of vacancies near the melting point was estimated at 0.032 per anion. A rise in pressure leads to a decrease in the diffusion coefficient and, respectively, a decrease in the conductance of the salt as a

result of the rise in the temperature of the transition to the superionic state [74, 75].

The special features of the diffusion processes discussed above, related to the presence of distributions of energies of stable and transition states, i.e. of an activation energy distribution, play an important role in the behavior of amorphous systems, since they determine the way in which irreversible and/or reversible structure relaxation proceeds. When relaxation is irreversible, partial annihilation of defects of different signs occurs and the free volume decreases slightly (free-volume outflow). The annihilation mechanism is connected with diffusion that proceeds according to the activation mechanism discussed above. On the other hand, reversible relaxation occurs because of the temperature dependence (or pressure dependence, and the like) of the short-range order, in particular, 'chemical short-range order,' which is defined in the simplest way as the ratio of the number of A–B pairs of nearest neighbors to this number in the disordered solid solution. One way to analyze the structure relaxation kinetics is to follow the temporal variations of physical properties, such as electrical resistance, thermal resistance, magnetic properties, enthalpy, rates of deformation under stress, and positron annihilation. This approach has been used to discover the wide activation energy spectra in amorphous alloys [76]. In the case of Zr–Ni–Cu alloys, the kinetics of reversible structure relaxation points to a narrow activation energy distribution near 1.1 eV and to a contribution of the cooperative mechanism at temperatures above 500 K [77]. Here relaxation is due to the regrouping of nickel and copper atoms. Since the characteristic structure relaxation times are long (e.g. ranging from 75 to 7000 s for the amorphous alloy $Fe_{40}Ni_{40}B_{20}$ [78]), direct simulation if such processes by the MD method is impossible.

4.2.4 Other variants of activated self-diffusion. The exchange mechanism of diffusion amounts to a direct exchange of the positions of two neighboring atoms in a single elementary event and is assumed to be highly improbable in the closely packed structure of metal alloys. The ring mechanism amounts to a simultaneous movement of a group of atoms in the form of a rotation of a triplet, quadruplet, etc. of nearest neighbors, in which movement each particle takes up the site occupied previously by another participant of the rotation. For instance, Divinski and Larikov [79] proposed that in the quasicrystalline intermetallic compounds AlMnSi and AlZnMg, six to ten atoms participate in the rotation of rings. Fam Khak Huang [80] simulated diffusion in a two-dimensional disordered lattice by the ring and exchange mechanisms. The lattice had 40×40 sites with a periodic boundary condition and a uniform (on a segment) distribution of energies ε_b of transition states with a standard deviation σ_b. The energies of the stable states were assumed constant. Three types of experiments were conducted in which the atoms move (1) only by the ring (A) mechanism, (2) only by the exchange mechanism (B), and (3) by both mechanisms A and B simultaneously. In A-calculations attempts were made to rotate a square with four atoms at the vertices. It was assumed that the squares of the grid rotate independently and that clockwise and counterclockwise rotations are equiprobable. After a certain number of steps the mean square displacement of the atoms was calculated. The mean equilibrium average time between two successive rotations was calculated by the method proposed in Ref. [51]. It was found that the correlation factors for both mechanisms monotonically decrease with temperature and that for equal values of σ_b/kT the factor F_B is smaller than F_A. Hence the correlation factor was dependent not only on temperature but also on the diffusion mechanism. This can be explained by the fact that at low temperatures two-site (mechanism B) and four-site (mechanism A) traps form in the system. The $\ln(D/D^*)$ vs. σ_b/kT curves are not linear and the slope of the curves increases with decreasing temperature. This leads to a temperature dependence of the activation energy. As in Ref. [51], the ratio D/D^* is greater than unity and increases with decreasing temperature.

When both mechanisms are activated, the reciprocal time between two diffusion events is almost equal to the sum of the reciprocal times for each mechanism. However, the diffusion coefficient in this case is larger than the sum of the coefficients for each mechanism. For instance, at $\sigma_{bA}/kT = \sigma_{bB}/kT = 5.2$ the ratio $s = D_{AB}/(D_A + D_B) = 5.45$. The reason is that the possibility of the atoms moving by two mechanisms reduces the concentration of traps and hence leads to an enhancement of the correlation factor, which now depends not only on temperature but also on the D_A-to-D_B ratio.

Fam Khak Huang et al. [81] simulated diffusion by the ring mechanism in a lattice with $10 \times 10 \times 10$ sites with periodic boundary conditions. They considered independent rotations of two types of ring: squares and rectangles. In all cases the mean square displacement of an atom was found to be proportional to the number of rotations, and the average real time between two rotations was found to be equal to the equilibrium value.

Thus, in diffusion by several possible mechanisms, the mechanisms interact, which increases the diffusion coefficient.

5. Diffusion along interstices of an amorphous system

5.1 One-component model systems

Fam Khak Huang and the present author [67, 82, 83] studied self-diffusion in models of amorphous one-component systems constructed at $T = 0$ by the continuous static relaxation (CSR) method with pair potentials of the type

$$u(r) = \varepsilon\left(\frac{r_0}{r}\right)^m \tag{28}$$

(i.e. in 'canonical structures' [84]) with $m = 6$, 18, 30 (686 particle in the main cube, and $r_0 = 0.1$ nm), in models of amorphous iron with the Pak–Doyama potential [85], and in several crystalline structures. In all cases periodic boundary conditions were employed. The diffusion of atoms of the system along interstices was investigated, so that the interaction potential between an interstitial atom and the other atoms was the same as between the atoms of the amorphous solid. At first the distributions of the energies of the stable and transition states were found. To this end the positions of the potential minima (interstices) and the routes from one interstice to the neighboring interstice were calculated. Finally, the diffusion coefficient for the interstitial atoms was calculated by the method of determining the velocity of drift initiated by an external field by Eqn (26). The calculations were done by the probability-field method with an external force incorporated in it.

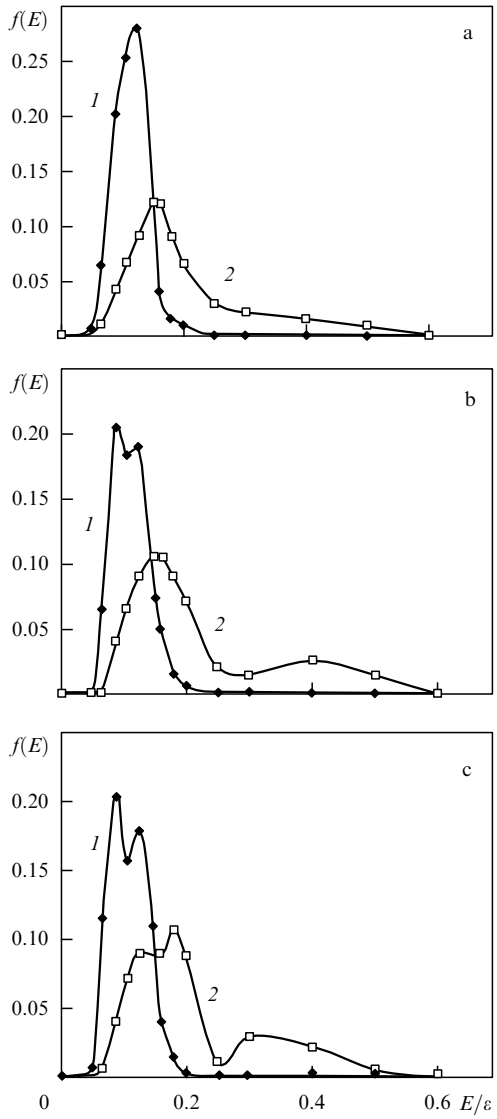

Figure 5. Distribution energies of the stable (curves *1*) and transition (curves *2*) states for diffusion in canonical structures with $m = 6$ (a), 18 (b), and 30 (c) [83].

Figure 5 depicts the distributions of the energies of stable and transition states in amorphous canonical structures with $m = 6$, 18, and 30. At $m = 18$ and 30, splitting of the first peaks for the stable states was detected. In all cases the dependence of the self-diffusion coefficients was found to be of Arrhenius type:

$$\ln D = -\mathrm{A} - \mathrm{B}\,\frac{\varepsilon}{kT}\,. \tag{29}$$

When the impurity – solvent potential is taken in the Pak – Doyama form, the pre-exponential factors $D_0 = \exp(-\mathrm{A})$ for BCC and FCC lattices, the amorphous iron model, and canonical structures prove to be very close, in the 0.015 to 0.029 $\mathrm{cm^2\ s^{-1}}$ range, and the factor B takes the following values:

System	BCC	a-Fe	$m = 6$	$m = 18$	$m = 30$	FCC
B	0.0602	0.0602	0.0628	0.0692	0.0693	0.0863

The values of the factor B for amorphous structures are between the values for BCC and FCC structures. This corresponds to a situation in which the average coordination numbers for the amorphous phase are between the coordination numbers for the BCC and FCC structures. Thus, the self-diffusion coefficient proves to be a monotonic function of the average coordination number.

5.2 Diffusion of hydrogen in amorphous alloys

The solubility of hydrogen in amorphous alloys based on hydride-forming metals (e.g. Pd, Zr, and Nb) amounts to several tens of percent and the enthalpy of solution of hydrogen in such alloys is negative (heat is released) [86]. These systems exhibit a strong dependence of some of the properties of the dissolved hydrogen (partial volume, dissolution heat, diffusion activation energy, and the pre-exponential factor) on hydrogen concentration. Deviations from the Sieverts law (when the solubility is proportional to the square root of the hydrogen pressure) have been recorded even at relatively low concentrations (0.2 – 0.4 at. %) [87]. In amorphous alloys of 3d-metal (Fe, Co Ni) – metalloid (B, P, Si) type the solubility of hydrogen, C_{H}, is much lower (of order 10^{-4} at. H/at.Fe at normal pressure [88]). For instance, Gritsenko et al. [88] found that in the amorphous metal alloy $\mathrm{Fe_{83}B_{17}}$ the dependence of C_{H} on $1/T$ is nonlinear, which suggests that there is a strong temperature dependence of the entropy and dissolution heat of hydrogen in the amorphous alloy (the dissolution heat increases from -5.66 kJ (g-at.)$^{-1}$ at 393 K to -0.55 at 573 K). The Sieverts law breaks down in this case. Gritsenko et al. [88] measured the diffusion coefficient for hydrogen in $\mathrm{Fe_{83}B_{17}}$. The dependence of $\ln D$ on $1/T$ was also found to be nonlinear, with the diffusion activation energy decreasing with increasing temperature. The average value of this activation energy in the 430 – 580 K interval is 29 kJ (g-at.)$^{-1}$, which places it between the activation energies in the BCC and FCC structures of iron (10 and 45 kJ (g-at.)$^{-1}$, respectively). However, the diffusion coefficient in the amorphous alloy $\mathrm{Fe_{83}B_{17}}$ is several orders of magnitude smaller than in iron. Contrary to such behavior, in the amorphous alloy $\mathrm{Fe_{78}B_{19}Si_3}$ a reduction in diffusion coefficient for hydrogen under crystallization has been discovered [89].

Toth et al. [90] studied the diffusion of hydrogen in the event of hydrogen desorption from the amorphous alloys $\mathrm{Zr-Ni-H}_x$. The desorption proceeds in two stages. The first one is very fast, and its mechanism has yet to be explained. The second one is of an activation nature with an activation energy $E = 0.32 \pm 0.04$ eV (the electrical resistance method) and 0.34 ± 0.02 eV (the spin-echo method).

These effects are caused by the presence in the alloy structure of positions for the hydrogen impurity with different stable-state energies. A large fraction of the hydrogen atoms is trapped by low-energy absorption centers and on heating to 523 K in vacuum remain in the 'bound' state. The trapping centers may be large pores, cavities and microcracks in which molecular hydrogen accumulates.

Lately the diffusion of hydrogen in amorphous silicon has attracted a lot of attention [91 – 98]. There are many indications of the presence of inhomogeneities in the structure of various types, which affect the nature of hydrogen diffusion. The activation energies found by the method of measuring the spin–lattice relaxation times (milliseconds are the characteristic values), are less by one order than those measured by the slower secondary-ion mass

spectroscopy method (times of the order of hours and days) [91]. Gaseous hydrogen trapped by micropores plays an important role here. Dozier et al. [92] found that, in diffusion in a-Si : H/a-Si : D bilayers, the hydrogen and deuterium atoms can move over distances not exceeding 100 A before they meet micropores and are trapped by them. Branz et al. [98] treated the problem of hydrogen diffusion in a system with single traps analytically. The results of their calculations are expressed in terms of the average time an impurity stays in a trap, τ. For short times ($t < \tau$), trapping effects manifest themselves in the concentration profile. For long times ($t > \tau$), the diffusion profile is ordinary but with an effective diffusion coefficient. The average path of a hydrogen atom before it is trapped decreases on an increase in illumination intensity and an increase in the annealing temperature [98].

However, Greim et al. [95] noted an increase in the rate of hydrogen diffusion in amorphous silicon films illuminated by intense light in the visible spectrum; probably, hydrogen atoms free themselves from the traps. Possibly, the problem of the effect of light is not so simple and several different processes participate in the given phenomenon.

The concentration of hydrogen is also important. As it increases from 1 to 19 at. %, the diffusion coefficient D_H increases by four orders of magnitude [92]. This agrees with the idea that the first impurities are trapped by the deepest traps (in our case, the unsaturated silicon bonds) and are the slowest to diffuse, while the impurities that follow are trapped by shallower traps, which have a weaker 'grip' on the impurity particles [94]. The limiting role of traps was noted by Beyer and Zastrow [96], who believe that hydrogen diffuses in an uncharged state and is trapped by intrinsic defects (free silicon bonds). Another small-sized impurity, lithium, diffuses in the form of Li^+ ions and is trapped primarily by negatively charged impurity ions or soluble hydrogen. At very low hydrogen concentrations (lower than 2×10^{19} at. cm^{-3}) the results differ strongly from those observed at ordinary concentrations above 10^{20} at. cm^{-3}. For instance, Roth et al. [97] found, for low concentrations, that $E = 2.70$ eV and that the pre-exponential factor $D_0 = 2.2 \times 10^4\ cm^2\ s^{-1}$. The high value of D_0 does not agree with the simple trap model. The situation becomes even more complicated if in the process of diffusion annealing there is structure relaxation. In this case D_H may be explicitly time-dependent (say, increase with the passage of time [93]).

A distribution of the energies of the stable states is accompanied by a distribution of the energies of the transition states. This may explain the deviations from the temperature dependence of the diffusion coefficient from the Arrhenius law [88, 99, 100].

Kirchheim [101] studied the diffusion of hydrogen in amorphous metal alloys analytically. The very fact that a trap for hydrogen can accommodate only one atom can be taken into account by using Fermi–Dirac statistics for the impurity atoms. The researcher derived an expression for the hydrogen diffusion coefficient that incorporated the width of the energy distribution for the impurity atoms at sites. It was found that at high hydrogen concentration the diffusion activation energy is lower than at low concentrations.

The distributions of the energies of the stable and transition states for hydrogen solutions in amorphous iron in comparison to hydrogen solutions in crystalline iron were analyzed in Refs [82, 83]. There the impurity–solvent interaction potential was chosen in the form of the Morse potential:

$$u(r) = \begin{cases} \varepsilon\{\exp[-2\alpha(r - r_0)] - 2\exp[-\alpha(r - r_0)]\}, & r < r^*, \\ 0, & r > r^*, \end{cases} \quad (30)$$

where $r_0 = 0.173$ nm, $r^* = 0.5$ nm, $\varepsilon = 0.22$ eV, and $\alpha = 13.4\ nm^{-1}$. Good agreement with the experimental data was achieved for the activation energies of hydrogen diffusion in the BCC and FCC structures of iron. At 700 K the diffusion coefficients were found to be equal to 6.1×10^{-4}, 1.0×10^{-7}, and $1.6 \times 10^{-5}\ cm^2\ s^{-1}$ for BCC, FCC, and amorphous iron, respectively.

A statistical calculation of the properties of diluted solutions of hydrogen in amorphous iron was carried out in Ref. [102]. The H–Fe interaction potential was chosen in the form (30). The activation energy of hydrogen diffusion in BCC and FCC iron and the entropy of hydrogen dissolved in the crystalline and liquid phases of iron were taken as the adjustable properties. The entropy of the dissolved hydrogen was established by calculating the frequencies of vibrations of the hydrogen atoms at sites by the formulas for a three-dimensional oscillator. The diffusion activation energy was found from the profile of the potential energy of a hydrogen atom along straight paths connecting two neighboring equilibrium positions in the computer model of amorphous iron or in an iron crystal. Wide distributions of the energies and vibration frequencies of hydrogen atoms in the stable states were found. In the crossover from the liquid phase to the amorphous, the distributions get narrower and are shifted to somewhat lower energies and higher frequencies.

At low temperatures the hydrogen atoms occupy the lowest energy positions possible, i.e. positions close in coordination to the O-positions in FCC iron (at the center of the elementary cell). In these positions the vibration frequencies of the hydrogen atoms are also the lowest. The presence of energy and vibration-frequency spectra leads to a strong temperature dependence of the entropy and the heat of dissolution of hydrogen in amorphous iron. At ~ 500 K the sign of the dissolution heat changes. The calculated values of the dissolution of hydrogen in amorphous iron are higher than in BCC iron over the entire region where the BCC phase exists [102].

The behavior of hydrogen in amorphous iron was also studied by Gritsenko et al. [103] by the Monte Carlo method. Earlier Yamamoto [104] constructed models of liquid and amorphous iron by using the MD and CSR methods and the Pak–Doyama pair potential. For the H–Fe pair the potential was chosen in the form of a fourth-degree polynomial, and the coefficients of the polynomial and the cutoff radius of the potential were selected according to the entropy, the dissolution heat, and the diffusion activation energy of hydrogen in crystalline BCC and FCC iron, and also according to the entropy, the dissolution heat, and the absolute value of the dissolution of hydrogen in liquid iron.

The H–Fe potential was then used to calculate the energy spectrum of the hydrogen atoms dissolved in amorphous iron. The spectrum turned out to be close to that found in Ref. [102]. The concentration of the equilibrium positions of interstitial hydrogen (~ 4.3 per iron atom) lies between the values for BCC and FCC iron. In the FCC crystal model, one equilibrium octahedral position per iron atom was found (with an energy of -2.17 eV). The energy of the lowest

hydrogen state in amorphous iron (−2.55 eV) is lower than that in the crystal iron lattice.

Gritsenko et al. [103] analyzed the geometry of the arrangement of atoms of amorphous iron surrounding hydrogen atoms for low-energy (L) and high-energy (H) equilibrium positions of the impurity particles.

For the L-positions, the packing of the iron atoms surrounding the hydrogen atoms is octahedral and smeared, which agrees with the fact that the coordination number is six. For H-positions, the peak in the angular distribution is close to 109°, which correlates with low coordination number. The Voronoi polyhedra built for the hydrogen atoms have a larger volume for L-positions (0.706 A^3) than for H-positions (0.448 A^3) and a much larger sphericity (0.446 against 0.204). However, one can encounter H-positions with very large Voronoi-polyhedron volumes. A similar picture is observed for FCC iron, where the volume of the low-energy octapores is much larger than that of tetrapores, which have a higher energy. Interestingly, the biggest pores in an amorphous matrix are not the most favorable from the standpoint of energy for the introduction of hydrogen. For L-positions, a relationship exists between the energy of the interstitial hydrogen atom and the volume of the corresponding Voronoi polyhedron. Such a relationship is absent for most H-positions. Large vacancy-like pores are not energetically advantageous for the introduction of atomic hydrogen [103].

The hydrogen diffusion coefficients for models of amorphous, BCC, and FCC iron were calculated in Ref. [83] by the probability-field method with an external force incorporated in the method (see above). The impurity – solvent interaction potential was chosen in the form (30) with $\varepsilon = 0.22$ eV, $\alpha = 13.4$ nm^{-1}, and $r^* = 0.173$. It was found that the distributions of energies of the stable and transition states are almost independent of the model density. These distributions are depicted in Fig. 6. The calculated parameters of the hydrogen diffusion in the different models are listed in Table 4.

Table 4. Parameters of hydrogen diffusion in amorphous iron.

Iron	Source	Diffusion parameters	
		D_0, 10^{-4} cm^2 s^{-1}	E, eV at.$^{-1}$
BCC-Fe	Model [83]	1.4	0.126
	Experiment [100]	22	0.0611 – 0.142
FCC-Fe	Model [83]	7.3	0.398
	Experiment [100]	100	0.334 – 0.521
Amorphous	Model [83]		
85.59 at. nm^{-3}		3.8	0.246
81.47 at. nm^{-3}		15	0.292
77.78 at. nm^{-3}		22	0.297

For BCC and FCC iron the calculated value of the activation energy E was found to be in good agreement with the experimental data. This suggests that the iron – hydrogen potential was chosen correctly. For amorphous-iron models, the value of E increases slightly as the model density decreases. For the pre-exponential factor, the discrepancy with the experimental data for crystals reaches a factor of ten, which is due to the difficulty of calculating the period of vibrations of a hydrogen atom near a stable state [83]. The calculated diffusion coefficient for hydrogen in amorphous iron is between the values for BCC and FCC iron. This is similar to the result obtained in Section 5.1 for self-diffusion in one-component systems.

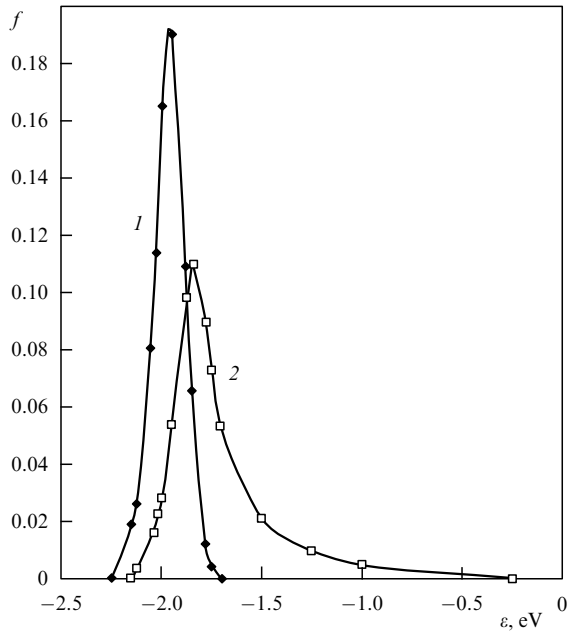

Figure 6. Distributions of energies of the stable (curve *1*) and transition (curve *2*) states for diffusion of hydrogen in the model of amorphous iron. The iron density is 85.6 at. nm^{-3} [83].

5.3 Diffusion of carbon along interstices of amorphous iron

Lancon et al. [106] calculated the coefficient of the diffusion of carbon along the interstices of an amorphous-iron model in which the diffusing impurity atoms were assumed to travel along tunnels between triples of neighboring solvent atoms. Knowing the impurity – solvent potential, one can calculate the activation-barrier heights and then find the diffusion mobility by the Monte Carlo method. It was found that in this approximation the Arrhenius law holds, and the calculated carbon diffusion coefficients were found to be larger than for FCC iron (by a factor of approximately 60 at 500 K).

6. Local inhomogeneities of an amorphous structure and the problem of 'defects.' Vacancies ('pores') in amorphous systems. The vacancy diffusion mechanism in amorphous metals

Initially researchers assumed that the existence of fairly stable large pores in amorphous solids (and in models of amorphous solids) was highly improbable. For instance, Bennett et al. [107] and Finney and Wallace [108] found that after one or several atoms are removed from the model of an amorphous solid with a Lennard–Jones potential and subsequent molecular-dynamics or static relaxation, the cavities almost disappear. However, in modeling a system of a covalent nature (with a three-body Keating potential, which was proposed for amorphous silicon type tetrahedral semiconductors), it was found that the pores are fairly stable. Later it was shown that the size and stability of pores depend on the interparticle interaction potential and the local surroundings of a pore. True, already in the illustrations in Ref. [109], after static relaxation of the amorphous iron model with a Johnson

potential one can clearly distinguish a well-defined large pore. Still later, the method of positron annihilation and later the method of small-angle x-ray scattering and electron microscopy made it possible to detect micropores, similar to vacancies in crystals, in real amorphous metal alloys (e.g., see Refs [110–113]). Kristiak [114] found that these 'quasivacancies' can combine into clusters. Limoge [115] analyzed the dependence of the diffusion coefficients on the hydrostatic pressure and found that the activation volume is approximately equal to the atomic volume. There are indications that on deformation the number of micropores ('quasivacancies') inside an amorphous metal alloy increases (this was established for $Ni_{60}Nb_{40}$ [116] and $Pd_{40}Ni_{40}P_{20}$ [117]), while on heating the number of such micropores decreases because of defect healing [118]. Micropores may generate microcracks in the amorphous alloy, which strongly affect the properties of the alloy [119]. The healing of micropores in the process of structure relaxation usually results in a slight compression of the solid, known as 'free-volume outflow.' As for the data on the effect of structure relaxation on micropores, they are quite contradictory, since this relaxation affects both the topological order and the chemical short-range order.

Usually, the analysis of pores in an amorphous structure is done on atomic models by calculating the radii of the hard spheres that can be embedded in the model without intersecting the atomic spheres [120, 121]. This yields a distribution of pores by their radii. Ahmadzadeh and Cantor [120] and Finney [121] investigated models of close packing of hard spheres and the system after its relaxation with Lennard-Jones or Morse type pair potentials. The behavior of pore type inhomogeneities in an amorphous structure was studied in Ref. [122] on 'canonical structure' models constructed with pair potential of the type (28). There the maximum value of the distance from a point inside the model to the nearest atom was determined. This distance (in units of $d = (V/N)^{1/3}$, where N is the number of particles in volume V) increases somewhat as the rigidity of the potential grows, from 0.827 at $m = 4$ to 0.886 at $m = 16$. For the hard-spheres model this distance is 0.884. This means that biggest pore has a diameter of about 0.66 of the radius of the sphere.

In models of amorphous iron with a Pak–Doyama potential, the maximum radii of the pores were 65–70 pm [10]. Under structural relaxation of the model these pores become somewhat smaller. Pores with a radius larger than 80 pm disappear in the CSR process and can be thought of as being removable structural defects of amorphous iron. The decrease in the maximum radii of the pores under structural relaxation has also been detected in the model of the amorphous alloy $Fe_{70}B_{30}$ [10].

Fam Khak Huang et al. [48, 123] studied pores in models of amorphous iron with the Pak–Doyama potential [there were 686 particles in the main cube, the density was 85.49 at. nm^{-3}, and the energy of the system varied from -1.371 (model A) to -1.385 eV at.$^{-1}$ (model B)]. The models were constructed by the CSR method and then some were annealed at 300 and 500 K by the Monte Carlo method. The pore size was determined by the method described above, and the radius of the atom was set at 131 pm. In model A, 146 pores with radii larger than 40 pm were discovered. Of these, 14 pores had radii larger than 60 pm and the largest pore had a radius of 82 pm. In the most stable model there were only 4 pores whose radii were larger than 60 pm. Large pores prove to be the unstable elements in the structure, and their removal under structural relaxation (as result of annealing by the Monte Carlo method at 300 and 400 K) reduces the energy of the system. In the process of relaxation, the sizes of individual pores may increase or decrease, and an initial shrinkage may be replaced by dilation (and vice versa), which is the consequence of collective atomic movements. Theoretically there can also be thermally activated formation of large pores with radii exceeding 80 pm, but due to its low probability this phenomenon was not observed in the computer experiment. The pore-size distributions obtained in Ref. [123] are depicted in Fig. 7.

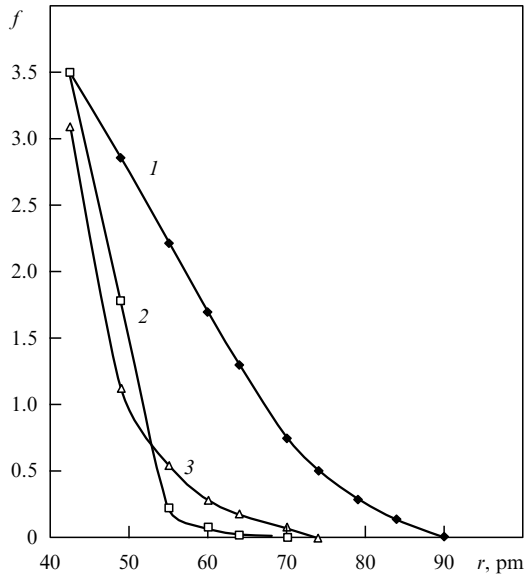

Figure 7. Pore size distributions for the model of liquid iron at 1900 K (curve *1*) and the models of amorphous iron with energies -1.371 (curve *2*) and -1.393 eV per atom (curve *3*) [122].

Pore type defects may also be encountered in models of amorphous alloys, especially those where the sizes of the component atoms differ substantially. For instance, in models of amorphous Fe_2Tb constructed at $T = 0$ by the CSR method, the Voronoi-polyhedra volume for the iron atoms amounted to 0.0152 ± 0.0034 nm^3 and that for the terbium atoms, to 0.0243 ± 0.0011 nm^3 [124]. A comparison with one-component amorphous systems shows that the spread in the Voronoi-polyhedra volumes and their sphericity are much larger in the case of the amorphous alloy Fe_2Tb. If we assume the radii of the iron and terbium atoms to be 124 and 178 pm, respectively, then at absolute zero the maximum radius of a pore in this model will be 134 pm. Twenty four pores with radii larger than 134 pm were found in the model. The largest pore could hold not only such impurity atoms as H, C, O, N, B, P, and Si but also the atoms Fe, Co, and Ni. Actually, such a pore is a vacancy for iron atoms. The emergence of such large vacancy type pores in models of amorphous alloys was observed earlier in the Fe–B system [125].

Fam Khak Huang et al. [126] did similar calculations of the distributions of pores for models of amorphous Co–P alloys. The researchers built distributions of the number of pores surrounding a phosphorus atom and the total volume of these pores. It was found that the number of large pores surrounding a phosphorus atom is much larger than the

number of large pores surrounding a boron atom (which is smaller than a phosphorus atom). More than that, the number of large pores surrounding a cobalt atom in Co – P alloys is larger than the corresponding number in Co – B alloys. The number of large pores increases with phosphorus concentration.

Van Ee et al. [127] used the MD method to study the dynamics of the size distribution of pores in models of amorphous $Ni_{81}B_{19}$ at temperatures above and below the glass transition (vitrification) temperature. As the temperature increases, the concentration of large pores (having seven or more neighbors) increases and the number of small pores (having six or fewer neighbors) decreases, and the pore size distribution broadens. Large pores may form in the process of merging of small pores and are a catalyst of diffusion by the cooperative mechanism.

Fam Khak Huang and the present author [123] defined a vacancy in an amorphous phase as a pore that is capable of repeatedly changing places with its neighboring atoms. The potential profile for the transition of an atom to the neighboring pore in the amorphous iron model has the form of an activation barrier only for pores whose radii exceed 80 pm. In model A (see above), only one such pore was detected. If static relaxation is carried out after the atom and the pore have changed places, the two remain in their new positions. In all other cases (for $R < 80$ pm) the displaced atom returns, under static relaxation to its initial position. Hence, in amorphous iron, pores with $R < 80$ pm play no important role.

For further studies of vacancies in amorphous iron models, several pores were created simultaneously by removing certain atoms whose separation was not smaller than 0.5 nm. Then static relaxation was carried out. This resulted in the formation of pores with radii from 60 to 110 pm. An analysis of the potential energy profiles showed that only pores with radii greater than 80 pm had normal activation barriers. Thus, the critical radius of 80 pm is the same for natural and artificial pores. The heights of the potential barriers for the atoms surrounding large pores vary between 0.4 and 2.7 eV. The height of the lowest barrier for each pore does not exceed 1.4 eV [123].

After a pore with a radius greater than 80 pm exchanges places with a neighboring atom, it will again have a radius greater than 80 pm, and so it is capable of changing places again, i.e. is a vacancy and does not disappear in the process of moving from place to place. However, the simulation described in Ref. [123] has shown that often the vacancy disappears after changing place (i.e. the vacancy dissipates) and lands in a 'sink.' The concentration of such sinks determines the average number of hops that a vacancy makes before it disappears, i.e. before it becomes an ordinary small pore.

The concentration of sinks was found in Ref. [123] by directly counting the number of sites at which artificially generated vacancies disappeared after changing places with an atom. For the models that were studied the atomic fraction of sinks decreases with the model energy (i.e. with the growth of model stability) from 0.53 to 0.125. It was found that a vacancy often disappears near the places where there is an atom with an (algebraically) enhanced energy of interaction with the neighbors.

If the sink concentration is α, the probability of a vacancy making exactly n hops and disappearing is $w_n = (1-\alpha)^n\alpha$. The average number of hops that a vacancy makes before it disappears is

$$n_{\mathrm{av}} = \frac{\sum_1^\infty n w_n}{\sum w_n} = \frac{1}{\alpha}\,. \tag{31}$$

Hence in the most stable B model a vacancy can make on average eight hops before it disappears.

Fam Khak Huang et al. [128] studied the self-diffusion of iron in an amorphous model containing 686 particles. Atoms were alternatively removed (one at a time) from the model, static relaxation was performed, and the energy of the system was calculated. The heights of the activation barriers in the transition of the neighboring atom to a pore were calculated. The result was an expression for the vacancy self-diffusion coefficient in amorphous iron in the form $D = 5.8 \times 10^{-3} \exp(-177.4\ \mathrm{kJ}/RT)\ \mathrm{cm^2\,s^{-1}}$. At 500 K, $D_{\mathrm{Fe}} = 8.1 \times 10^{-20}\ \mathrm{cm^2\ s^{-1}}$ (a computer calculation). The experimental data for the alloy $Fe_{40}Ni_{40}P_{14}B_6$ have a large spread. At 500 K, $D_{\mathrm{Fe}} = 9.5 \times 10^{-18}\ \mathrm{cm^2\ s^{-1}}$ (the data of Shuehmacher and Guiraldenq [129]) and $4.5 \times 10^{-18}\ \mathrm{cm^2\ s^{-1}}$ (data of Valenta et al. [130]). The fact that the experimental data exceed the calculated results is probably due to the presence in the initial amorphous alloy of nonequilibrium vacancies or to other diffusion mechanisms.

Ultimately, Fam Khak Huang et al. [48, 123] proposed the following scheme for diffusion in an amorphous solid by the vacancy mechanism. First, as a result of a thermal fluctuation, a large pore appears. Then the pore diffuses, changing places with neighboring atoms and making on average $1/\alpha$ hops. After that the vacancy lands in a sink and becomes a relatively small pore, which does not participate in the process of changing places.

In the case of crystalline solids rapidly hardened at high temperatures, the real vacancy concentration may be much higher than the equilibrium concentration. On the other hand, in amorphous metals the nonequilibrium vacancies (large pores) perish in the sinks after a few hops. Hence there is a high probability that these vacancies will manifest themselves only in the initial stages of diffusion, precisely, in the structure relaxation process. Subsequently, largely equilibrium vacancies remain, and these are formed in the process of thermal activation. Sinks may also be generated by fluctuations.

What is important is that in models of amorphous structures single pairs aggregate into larger formations consisting of ten or more spheres [131 – 134]. Medvedev [134] built Voronoi polyhedra and did an analysis in which the difference in the sizes of the component atoms, geometrical balls, was taken into account explicitly. A computer hard-spheres model was used to calculate the distribution of the 'passage radius' R_b, i.e. the radius of a ball that can pass without clearance between a neighboring triplet of balls of the model. The presence of large R_b is an indication that there are large pores in the system. By 'coloring' the bonds in the Voronoi grid starting from those that have the smallest values of the passage radius one can finally obtain a percolation cluster. All colored bonds will have passage radii that are no smaller than a certain value R_c, which is reached at the moment that percolation emerges. A test sphere of radius $\leqslant R_c$ can be guided along all these bonds of the grid, including the path through the same along the percolation cluster. Medvedev [134] found that the penetrability of the system increases with the difference in the radii of the atoms, although the packing factor remains approximately the same.

The reason is that the presence of larger atoms (balls) leads to the formation of still larger pores.

The behavior of vacancies in amorphous globules consisting of 1600 atoms with a Lennard-Jones pair potential was studied in Refs [68, 135], where the migration of vacancies was also investigated by the Monte Carlo method. A large spread in the heights of the activation barriers for the transition of an atom to a neighboring vacancy was discovered. In the process of self-diffusion, a vacancy prefers to move along paths with barriers of minimum height.

Delaye and Limoge [136] also analyzed the behavior of vacancies in the amorphous phase with the Lennard–Jones pair potential. They found that the formation energies and the heights of the activation barriers have wide distributions. Their calculations showed that the vacancy self-diffusion coefficient in the amorphous phase can be larger than in a crystal with the same pair potential by a factor of approximately 10^5.

The same researchers [137, 138] used the MD method (864 and 10976 atoms in the main cube, the temperature was varied between absolute zero and 10 K) to study vacancy-like defects in glasses with the Lennard–Jones potential. Atoms were removed (one at a time) from the system and relaxation was carried out. Here, too, as in Refs [48, 123], three possible modes of behavior were discovered: (1) relaxation of the surrounding region with the vacancy being conserved; (2) one of the neighboring atoms hops into the vacancy, and this is accompanied by the transition of the first coordination sphere surrounding the former vacancy; and (3) the vacancy collapses and its free volume outflows to the surface of the glass. The outcome of the event was not related in any definite manner to the level of local shear stresses or to the extent to which the nearest surroundings resemble an icosahedron, although a low level of local pressure or a high sphericity of the surroundings probably stabilizes the vacancy. Vacancy collapse is facilitated by high local pressure and low sphericity. Irrespective of the size of the system, vacancy collapse is observed, on the whole, in 25% of the chosen sites (these were the sinks for the vacancy), in 10 to 30% of the cases the vacancy remained stable, and in the remaining cases one of the neighboring atoms hopped into the vacancy. Sometimes, however, an intermediate case, which does not fit this classification, was observed.

According to Delaye and Limoge [138], vacancies may appear at the sites of the amorphous phase that are sinks, may migrate to other sinks and disappear there, and the like. To make these processes more graphic, the researchers simulated the processes by reversing the time in the MD experiment after the vacancy had collapsed (before the collapse the vacancy did several hops from its initial position). They were able to restore the order of the migration process from the initial site to the sink. Delaye and Limoge [138] also calculated the distributions of the energies of formation of vacancies and the heights of the activation barriers for various models. For instance, at an average energy of vacancy formation of 0.062 eV, the observed distribution extended from 0.034 to 0.08 eV. The lower the local pressure, the higher the formation energy. The volume of stable vacancies amounts to 35 to 80% of the volume per atom. The heights of the activation barriers extended from 0.0055 to 0.118 eV (0.067 eV in FCC argon at absolute zero), i.e. the barriers can be much higher or much lower than those in the crystal. The vacancy formation entropy was calculated by the frequency spectra; it varies for different sites from $2.1k$ to $8.0k$, where k is Boltzmann's constant and is smaller, the larger the change in volume in vacancy formation. The vacancy formation heat is proportional to the change in the volume in the process of vacancy formation, with the proportionality factor coinciding with the value for FCC argon.

Delaye and Limoge [138] estimated the self-diffusion coefficient in amorphous argon assuming that the effects of the distribution of the energies of the stable and transition states balance each other. In this case the ratio of the self-diffusion coefficients in the amorphous and crystalline states is given by the formula

$$\frac{D_{\text{am}}}{D_{\text{cryst}}} = \exp\left(\frac{\Delta S_{\text{f}}}{k}\right) \exp\left[-(\Delta H_{\text{f}} + \Delta H_{\text{act}})\right], \tag{32}$$

where ΔS_{f}, ΔH_{f}, and ΔH_{act} are the differences between the formation entropies, formation heats, and vacancy activation energies in the amorphous phase and the crystal. Such a simplified approach yields the value $D_{\text{am}}/D_{\text{cryst}} \cong 10^8$ for argon at 25 K, which corresponds to the observed values for metallic glasses at $T \cong T_{\text{m}}/3$.

Thus, the above research shows that in disordered systems of the type of an amorphous metal alloy there can be a quasivacancy mechanism of diffusion that operates via activated formation of pores (quasivacancies) and a further change of places between the pores and the neighboring atoms. What makes this mechanism different from the vacancy mechanism in crystals is that (a) large pores are generated in special positions (sources), which are defective from the standpoint of structure, via thermal or another type of activation; (b) the quasivacancies are of different sizes; (c) pores whose sizes are smaller than a certain critical value lose their ability to migrate; (d) the collapse of a quasivacancy occurs not on macroscopic defects, as it does in a crystal, but in the defective sections of the amorphous structure, or vacancy sinks; and (e) there is a 'mean free path' of a vacancy before collapse, and the length of this path is determined by the sink concentration. As a result of thermal fluctuations, sources and sinks may appear in different parts of the system.

7. Modeling diffusion in loose systems

As noted earlier, three-body potentials, which incorporate not only the distances between the particles but also the valence (azimuthal) angles in the triangles formed by the triplets of nearest neighbors, are used in the construction of models of amorphous or liquid matter with covalent bonds (e.g. Si, Ge, and CdTe).

One must bear in mind that the inclusion of the Stillinger – Weber potential does not automatically lead to the construction of a covalent amorphous model. For instance, it is practically impossible to construct such a model on the basis of a random initial arrangement of atoms in the main cube. The reason is that in the final state the coordination number for almost all particles must be equal to four. Hence, in constructing covalent models a key issue is the initial arrangement of the atoms, which is usually chosen to be ordered and is then relaxed in one manner or another. In modeling the liquid phase, three-body corrections play an insignificant role, since the coordination numbers in the liquid state of silicon type substances are substantially larger than four and the structure of the three-body correction to the potential does not correspond to the topology of the real system.

A characteristic feature of real loose structures is the presence of a large number of inner cavities (pores) connected by channels, which may serve as rapid diffusion paths. For instance, experiments have shown that an Au impurity in amorphous Ge and Pt in a-Si diffuse at 673 – 923 K along interstices. Here they can be trapped by traps of various depths [139], similar to the case of hydrogen diffusion (see Section 5.2). The presence of large pores is also a characteristic feature of models of ionic and covalent noncrystalline systems.

The pore size distribution in models of amorphous silica constructed by the Monte Carlo method has been calculated, for example, by Chan and Elliott [140]. In ionic MD models of SiO_2 glasses containing 3000 atoms in the main cube, there were 3.1×10^{21} pores cm^{-3} sufficient to contain an He atom of radius 1.28 A, and 1.8×10^{21} pores cm^{-3} that were capable of incorporating a neon atom of radius 1.38 A [141] (a β-crystobalite crystal contains 2.18×10^{22} pores per cubic centimeter with a radius of 1.62 A per atom). Taraskin et al. [142] made a thorough study of the shape of the pores in SiO_2 models (648 particles) constructed with allowance for the three-body interaction. The researchers discovered the effect of pore grouping into more complicated, irregularly shaped 'branches' consisting of 10 to 20 pores, although most pores are single entities. Crossing each other, the 'branches' form 'trees.' The distance between the ends of long branches (containing more than three pores) increases as a power-law function of the number of pores with an exponent close to 0.82. The shape of the longest pores is close to linear. Obviously, the arrangement of the pores is important from the viewpoint of the diffusion mechanism (the presence of easy diffusion paths, the percolation aspect, and the like). The filling of these cavities by atoms of He, Li, or Na may dramatically change the shape of the first sharp peak (the precursor peak) in the structure factor of silica [143].

Computer data on the mechanisms of diffusion in models of loose noncrystalline systems are scant. Molecular dynamics calculations show that in the equilibrium-liquid region the self-diffusion coefficients for particles in ionic models and in models of liquid silicon and germanium are (in order of magnitude) 10^{-5} cm^2 s^{-1} and higher, but rapidly decrease on cooling to minimum values that can still be measured (of order 10^{-6} cm^2 s^{-1}), and then practically vanish. For instance, such was the result for KCl and $ZnCl_2$ [42]. Small ions (Li^+) diffuse faster than large ions [144]. Despite the cooperative diffusion mechanism in liquid-oxide models, Soules [145] described the temperature dependence of the self-diffusion coefficients for ions in SiO_2, B_2O_3, $Na_2O \cdot SiO_2$ and BeF_2 by the Arrhenius formula with activation energies close to the experimental values.

Balasubramanian and Rao [146] and Huang Chengde and Cormack [147] detected the preferable paths of migration of the fairly mobile ions Na^+, K^+, etc. through tunnels formed by overlapping pores between tetrahedral SiO_4 groups in models of alkali silicate glasses constructed by the MD method. In real complex silicate glasses, the competition between ions of different alkali metals leads to the appearance of anomalies in the diffusion mobility and the related electrical conductance of the glasses; these anomalies are represented by minima in the concentration dependence (the polyalkaline effect). For instance, in $xLi_2O \cdot (1-x)Na_2O \cdot 2SiO_2$ glasses, the conductance passes through a minimum at $x = 0.5$ [148]. At high temperatures, the polyalkaline effect is suppressed, probably, in connection with the easier relaxation of the anions. The MD method makes it possible to reproduce the polyalkaline effect on models by using specific interionic interaction potentials [146, 147].

A characteristic feature of ionic and ionic-covalent systems is the formation of large complex ions (of the SiO_4^{4-} type in silicates), which in view of their high stability may diffuse in the melt as an integral whole. For instance, in modeling ion transport in the melts of cryolite – Al_2O_3 [149] and $CaF_2 - Al_2O_3$ [150] systems in an external electric field, the researchers found that aluminum ions are dragged by the surrounding oxygen ions to the anode in the first case; the effect was just the opposite in the second case. The direction of migration in the field is determined by the structure and degree of stability of the first coordination spheres surrounding the ions. The Al – O pairs proved to have the longest lifetime, while in the absence of oxygen the Al – F pairs proved to have the longest lifetime. When aluminum oxide is added to fluoride, the oxygen ions replace fluorine in the first coordination sphere of the aluminium ion, and the fluorine ions lose their ability to drag the aluminum particles in the transport process.

8. Conclusion

We have discussed the results of computer simulation of diffusion processes in disordered systems for the two main diffusion mechanisms: cooperative (drift) and activation. For the first mechanism we can calculate with good accuracy (with an error of several percent) the self-diffusion coefficients for the particles of the system, provided that the interparticle interaction potentials are known. Calculating the potentials proper proves to be the most difficult problem. We also found that a detailed analysis of the cooperative mechanism is possible if the diffusion coefficients are larger than 10^{-6} cm^2 s^{-1} and that for smaller values of D the MD method proves to be of little use. Possibly, the study of large models incorporating $10^4 - 10^6$ particles will make it possible to move into the $D \sim 10^{-8} - 10^{-9}$ cm^2 s^{-1} range. The study of this mechanism for even stronger supercooling will require new theoretical approaches and calculation algorithms.

The main problems related to the activation mechanism of diffusion along interstices and the vacancy (or quasivacancy) mechanism in dense disordered systems appear to have been developed fairly thoroughly. The key factor is the presence of distributions of the energies of the stable and transition states. The distributions can be calculated, at least in principle, if we know the interparticle interaction potentials. Knowing these distributions, we can calculate the average time that a particle stays at a site and the correlation factor, which can then be used to calculate the self-diffusion coefficient for a component. We can also find the activation energy spectrum, which plays a central role in structure relaxation processes. The number of such calculations performed so far is clearly insufficient.

One must bear in mind that atomic models of amorphous metals that contain only thousands of particles can produce incorrect results when used to described what is known as medium-range order (on the scale of several nanometers or several tens of nanometers). This type of order is often observed in amorphous alloys, manifesting itself in the form of singularities in the small-angle region of the structure factor. Studying diffusion on such scales requires models of amorphous metal alloys that contain tens of thousands of

atoms (incidentally, modern medium-power computers can already handle such models).

The structure of loose disordered systems, such as covalent, ionic, and with an intermediate type of bonding, and the diffusion mechanisms for such systems appear to be more diverse than in the case of metal alloys. The research done so far in this field suggests that the presence of inner cavities (pores), the size distribution of the pores, the nature of pore overlap, the formation of easy paths for diffusion, and the mutual effect of rapidly diffusing ions play an important role. Far less studied is the behavior of the particles that form the fixed (more precisely, almost immobile) frame and are coupled by strong covalent bonds (as in amorphous silicon) or the strong Coulomb interaction (as in silica). The methods of theoretical analysis of diffusion processes in such systems have to be developed more thoroughly. However, in this case, too, the main diffusion mechanisms are the cooperative (for the liquid state) and the activation (in the glassy state). As in the case of dense systems, the transition from one mechanism to the other takes place in a region of diffusion coefficients (temperatures) that cannot be studied directly by the MD method.

References

1. Raetzke K, Hueppe P W, Faupel F *Key Eng. Mater.* (*Amorphous Metallic Materials*) **81–83** 579–582 (1993)
2. Murata M, Mizoguchi T *Key Eng. Mater.* (*Amorphous Metallic Materials*) **81–83** 297–302 (1993)
3. Bottiger J, Chechevin N G, Karpe N, Krog J P *Nucl. Instrum. Methods Phys. Res. B* **85** (1–4) 206–215 (1994)
4. Mehrer H, Rummel G "Diffus. Amorphous Mater.", in Proc. Int. Symp. 1993 (Eds H Jain, D Gupta) *Miner. Met. Mater. Soc.* (Publ. 1994) p. 163–176
5. Larikov L N *Metallofiz.* **15** (4) 54 (1993)
6. Larikov L N *Metallofiz.* **15** (8) 3 (1993)
7. Bokshteĭn B S, Karpov I V, Klinger L M *Izv. Vyssh. Uchebn. Zaved. Chernaya Metallurgiya* (11) 87 (1985)
8. Binder K (Ed.) *Monte Carlo Methods in Statistical Physics* (Berlin: Springer-Verlag, 1979) [Translated into Russian (Moscow: Mir, 1982)]
9. Heerman D W *Computer Simulation Methods in Theoretical Physics* (Berlin: Springer-Verlag, 1986) [Translated into Russian (Moscow: Nauka, 1990)]
10. Belashchenko D K, Tomashpol'skiĭ M Yu *Izv. Akad. Nauk SSSR Metally* (6) 137 (1987) [*Russ. Metallurgy* (6) 139 (1987)]
11. Polukhin V A, Vatolin N A *Modelirovanie Amorphnykh Metallov* (Modeling Amorphous Metals) (Moscow: Nauka, 1985)
12. Valuev A A, Norman G E, Podlipchuk V Yu "The molecular dynamics method: theory and applications", in *Matematicheskoe Modelirovanie. Fiziko-Khimicheskie Svoĭstva Veshchestva* (Mathematical Modeling. Physicochemical Properties of Matter) (Eds A A Samarskiĭ, N N Kalitkin) (Moscow: Nauka 1989)
13. Belashchenko D K *Usp. Khim.* **66** 811 (1997)
14. Polukhin V A, Ukhov V F, Dzugutov M M *Komp'yuternoe Modelirovanie Dinamiki i Struktury Zhidkikh Metallov* (Computer Simulation of the Dynamics and Structure of Liquid Metals) (Moscow: Nauka, 1981)
15. Belashchenko D K *Struktura Zhidkikh i Amorfnykh Metallov* (Structure of Liquid and Amorphous Metals) (Moscow: Nauka, 1985)
16. Vatolin N A, Kibanova E A, Polukhin V A *Dokl. Ross. Akad. Nauk* **356** 57 (1997)
17. Holender J M, Morgan G J *J. Phys.: Cond. Matter* **3** 7241 (1991)
18. Nakano A, Kalia R K, Vashishta P *J. Non-Cryst. Solids* **171** (2) 157 (1994)
19. Car R, Parrinello M *Phys. Rev. Lett.* **55** 2471 (1985)
20. Kresse G, in *Liquid and Amorphous Metals. 9th Int. Conf. Chicago, USA, Aug. 27–Sept. 1 1995*. Theses, p. 29
21. Costa Cabral B J, Martins J L, in *Liquid and Amorphous Metals. 9th Int. Conf. Chicago, USA, Aug. 27–Sept. 1 1995* Theses, p. 143
22. Kresse G, in *6th Int. Conf. on the Structure of Non-Crystalline Materials* (*NCM6*). *Praha, Aug. 29–Sept. 2 1994*. Abstracts, p. 107
23. Seifert K, Hafner J, Kresse G, in *Liquid and Amorphous Metals. 9th Int. Conf. Chicago, USA, Aug. 27–Sept. 1 1995*. Theses, p. 64
24. Yonezawa F, Tanikawa H, in *Liquid and Amorphous Metals. 9th Int. Conf. Chicago, USA, Aug. 27–Sept. 1 1995*. Theses, p. 43
25. Costa Cabral B J, Cordeiro M N D S, Telo da Gama M M *J. Phys.: Cond. Matter*. **3** 5615 (1991)
26. Costa Cabral B J, Martins J L, in *Liquid and Amorphous Metals. 9th Int. Conf. Chicago, USA, Aug. 27–Sept. 1 1995*. Theses, p. 144
27. Kirchhoff F, Holender J M, Gillan M J, in *Liquid and Amorphous Metals. 9th Int. Conf. Chicago, USA, Aug. 27–Sept. 1 1995*. Theses, p. 15
28. Pusztai L, Svab E *J. Phys.: Cond. Matter* **5** 8815 (1993)
29. Lamparter P, Steeb S *J. Non-Cryst. Solids* **192–193** 578 (1995)
30. Pusztai L, Gereben O *J. Non-Cryst. Solids* **192–193** 640 (1995)
31. Mendelev M I, Belashchenko D K, Ishmaev S N *J. Non-Cryst. Solids* **205–207** 888 (1996)
32. Mendelev M I *J. Non-Cryst. Solids* **223** 230 (1998)
33. Belashchenko D K *Metally* (4) 101 (1998)
34. Navarra G et al., in *6th Int. Conf. on the Structure of Non-Crystalline Materials (NCM6). Praha, Aug. 29–Sept. 2 1994*. Abstracts, p. 197
35. Woodcock L V *J. Chem. Soc. Faraday Trans. II* **72** 1667 (1976)
36. Angell C A, Clarke J H R, Woodcock L V, in *Adv. in Chemical Physics* (Eds I Prigogine, S A Rice) Vol. 48 (New York: Wiley, 1981) p. 397
37. Tsuneyuki S, in *Molecular Dynamics Simulations* (Springer Series in Solid-State Sciences, 103, Ed. F Yonezawa) (Berlin: Springer-Verlag, 1992) p. 78
38. Tsuneyuki Sh, Matsui Y *Phys. Rev. Lett.* **74** 3197 (1995)
39. Swalin R A *Acta Metall.* **7** 736 (1959)
40. Mathiak G, Griesche A, Kraatz K H, Frohberg G, in *Liquid and Amorphous Metals. 9th Int. Conf. Chicago, USA, Aug. 27–Sept. 1 1995*. Theses, p. 126
41. Kimura M, Yonezawa F "Computer Glass Transition", in *Topological Disorder in Condensed Matter. Proc. 5th Taniguchi Int. Symp., Shimoda, Japan, Nov. 2–5, 1982* (Eds F Yonezawa, T Ninomiya) (Berlin, 1983) p. 80
42. Woodcock L V, Angell C A, Cheeseman P *J. Chem. Phys.* **65** 1565 (1976)
43. Pavlov V V *O 'Krizise' Kineticheskoĭ Teorii Zhidkosti i Zatverdevaniya* (On the 'Crisis' of the Kinetic Theory of Liquids and Solidification) (Ekaterinburg: Izd. Ural. Gos. Gornometallurg. Akad., 1997)
44. Chen H S et al. *Appl. Phys. Lett.* **32** 461 (1978)
45. Bokshteĭn B S et al. *Fiz. Met. Metalloved.* **51** 561 (1981)
46. Hivatari Y J *Chem. Phys.* **76** 5502 (1982)
47. Akhiezer I A, Davydov L N, Spol'nik Z A "Samosoglasovannaya model' stekol metall–metalloid" ("Self-consistent model of metal–metalloid glasses") Preprint KhFTI 87-36 (Kharkov: Khar'kovskiĭ Fizikotekhn. Institut Ukrainskoĭ Akad. Nauk, 1987)
48. Fam Khak Huang, Belashchenko D K, Nguen Suan Tu *Izv. Vyssh. Uchebn. Zaved. Chernaya Metallurgiya* (11) 152 (1989)
49. Fam Khak Huang, Belashchenko D K, Nguen Suan Tu "Modelirovanie samodiffuzii v amorfnom zheleze" ("Modeling of self-diffusion in amorphous iron"), manuscript deposited at the All-Union Institute of Scientific and Technical Information, 4211-B89, Moscow (1989)
50. Belashchenko D K *Fiz. Met. Metalloved.* **53** 1076 (1982)
51. Belashchenko D K et al. *Izv. Akad. Nauk SSSR Metally* (2) 57 (1986)
52. Kijek M, Ahmadzadeh M, Cantor B, in *Proc. Int. Conf. Met. Glas.: Sci. and Technol., Budapest, 1980* Vol. 2 (Budapest, 1981) p. 397
53. Belashchenko D K, Fam Khak Huang *Izv. Vyssh. Uchebn. Zaved. Chernaya Metallurgiya* (11) 89 (1986)
54. Limoge Y, Bocquet J L *Phys. Rev. Lett.* **65** 60 (1990)
55. Keller J U *Z. Naturforsch. A* **26** 1539 (1971)
56. Haus J W, Kehr K W "Diffusion in regular and disordered lattices" *Phys. Rep.* **150** 263 (1987)
57. Akhiezer I A, Davydov L N "O diffuzii v neuporyadochennykh metallakh" ("On diffusion in disordered metals") Preprint KhFTI

89-16 (Kharkov: Khar'kovskiĭ Fizikotekhn. Institut Ukrainskoĭ Akad. Nauk, 1989)
58. Gorbunov D A, Klinger L M *Fiz. Met. Metalloved.* **61** 1084 (1986)
59. Belashchenko D K, Fam Khak Huang *Fiz. Met. Metalloved.* **57** 1050 (1984)
60. Sinaĭ Ya G *Teor. Veroyatn. Primen.* **27** 247 (1982)
61. Obukhov S P *Pis'ma Zh. Eksp. Teor. Fiz.* **39** 21 (1984) [*JETP Lett.* **39** 23 (1984)]
62. Zwanzig R *J. Stat. Phys.* **28** 127 (1982)
63. Kehr K W, Richter D, Swendsen R H *J. Phys. F* **8** 433 (1978)
64. Belashchenko D K, Fan Suan Hien *Izv. Vyssh. Uchebn. Zaved. Chernaya Metallurgiya* (1) 94 (1988)
65. Fam Khak Huang, Belashchenko D K, Nguen Hyu Hung *Izv. Vyssh. Uchebn. Zaved. Chernaya Metallurgiya* (7) 153 (1989)
66. Fam Khak Huang, Belashchenko D K, Vo Van Hoang *Izv. Vyssh. Uchebn. Zaved. Chernaya Metallurgiya* (9) 153 (1988)
67. Fam Khak Huang, Belashchenko D K *Izv. Vyssh. Uchebn. Zaved. Chernaya Metallurgiya* (1) 65 (1990)
68. Belashchenko D K, Fam Khak Huang *Izv. Vyssh. Uchebn. Zaved. Chernaya Metallurgiya* (1) 149 (1983)
69. Kirkpatrick S *Rev. Mod. Phys.* **45** 574 (1973)
70. Belashchenko D K, Vo Van Hoang *Izv. Vyssh. Uchebn. Zaved. Chernaya Metallurgiya* (5) 54 (1990)
71. Limoge Y, Bocquet J L *Diffus. Defect Data A* **95 – 98** (Pt. 2) 1153 (1993)
72. Waseda Y *Prog. Mater.* **26** 1 (1981)
73. Rahman A *J. Chem. Phys.* **65** 4845 (1976)
74. Gillan M J, Dixon M *J. Phys. C* **13** 1901 (1980)
75. Dixon M, Gillan M J *J. Phys. C* **13** 1919 (1980)
76. Haruyama O, Asahi N, in *6th Int. Conf. on the Structure of Non-Crystalline Materials* (*NCM6*). *Praha, Aug. 29 – Sept. 2 1994*. Abstracts, p. 119
77. Ming Mao, Altounian Z, in *Liquid and Amorphous Metals. 9th Int. Conf. Chicago, USA, Aug. 27 – Sept. 1 1995*. Theses, p. 62
78. Csach K et al., in *9th Int. Conf. on Rapidly Quenched and Metastable Materials* (*RQ9*). *Bratislava, Aug. 25 – 30, 1996*. Book of Abstracts, p. 124
79. Divinski S V, Larikov L N, in *Liquid and Amorphous Metals. 9th Int. Conf. Chicago, USA, Aug. 27 – Sept. 1 1995*. Theses, p. 169
80. Fam Khak Huang "Modelirovanie diffuzii v dvumernoĭ neuporyadochennoĭ sisteme po kol'tsevomu i obmennomu mekhanizmam" ("Modeling of diffusion in a two-dimensional disordered system by the ring and exchange mechanisms"), manuscript deposited at the All-Union Institute of Scientific and Technical Information, 4629-B89, Moscow (1989)
81. Fam Khak Huang, Belashchenko D K, Nguen Hyu Hung "Modelirovanie diffuzii v neuporyadochennykh reshetkakh" ("Modeling of diffusion in disordered lattices"), manuscript deposited at the All-Union Institute of Scientific and Technical Information, 4628-B89, Moscow (1989)
82. Fam Khak Huang, Belashchenko D K *Izv. Vyssh. Uchebn. Zaved. Chernaya Metallurgiya* (3) 107 (1990)
83. Fam Khak Huang, Belashchenko D K *Izv. Akad. Nauk SSSR Metally* (3) 206 (1990) [*Russ. Metallurgy* (3) 201 (1990)]
84. Belashchenko D K *Fiz. Met. Metalloved.* **63** 665 (1987)
85. Belashchenko D K *Fiz. Met. Metalloved.* **60** 1076 (1985)
86. Stolz U et al. *J. Less-Common Met.* **103** (1) 81 (1984)
87. Nakamura K, Ber. Bunsenges *Phys. Chem.* **89** (1) 191 (1985)
88. Gritsenko A B, Andreev L A, Belashchenko D K *Fiz. Met. Metalloved.* **67** 972 (1989)
89. Albertini L B, Rodriques J A *Congr. Anu.-Assoc. Bras. Met. Mater* (1992)
90. Toth J et al. *J. Alloys Compd.* **23** (1 – 2) 334 (1995)
91. Hari P, Taylor P C, Street R A *J. Non-Cryst. Solids* **198 – 200** 52 (1996)
92. Dozier W D et al. *Mater. Res. Soc. Symp. Proc.* (*Amorphous Silicon Technology* -1992) **258** 401 (1992)
93. Shinar R et al. *Mater. Res. Soc. Symp. Proc.* (*Amorphous Silicon Technology*-1992) **258** 419 (1992)
94. Santos P V, Jackson W B *Mater. Res. Soc. Symp. Proc.* (*Amorphous Silicon Technology*-1992) **258** 425 (1992)
95. Greim O et al. *Solid State Commun.* **88** 583 (1993)
96. Beyer W, Zastrow U *J. Non-Cryst. Solids* **164 – 166** 289 (1993)
97. Roth J A et al. *Mater. Res. Soc. Symp. Proc.* (*Amorphous Silicon Technology*-1993) **297** 291 (1993)
98. Branz H M et al. *Mater. Res. Soc. Symp. Proc.* (*Amorphous Silicon Technology*-1993) **297** 279 (1993)
99. Richards P M *Phys. Rev. B* **27** 2059 (1983)
100. Kirchheim R, Sommer F, Schluckebier G *Acta Metall.* **30** 1059 (1982)
101. Kirchheim R *Acta Metall.* **30** 1069 (1982)
102. Gritsenko A N, Belashchenko D K *Fiz. Met. Metalloved.* **65** 1045 (1988)
103. Gritsenko A N, Belashchenko D K, Kosov I N *Fiz. Met. Metalloved.* (2) 57 (1991)
104. Yamamoto R et al. *J. Phys. F* **8** L179 (1978)
105. Belashchenko D K, Ginzburg A S *Zh. Eksp. Teor. Fiz.* **115** 50 (1999) [*JETP* **88** 28 (1999)]
106. Lançon F et al. *J. Phys. F* **15** 1485 (1985)
107. Bennett C H et al. *Philos. Mag. A* **40** 485 (1979)
108. Finney J L, Wallace J *J. Non-Cryst. Solids* **43** 165 (1981)
109. Egami T, Maeda K, Vitek V *Philos. Mag. A* **41** 883 (1980)
110. Nasu T et al. "A positron annihilation study of the evolution of amorphization in Nb_3Sn by mechanical attrition", in *7th Int. Conf. on the Structure of Non-Crystalline Materials* (*NCM7*). *September 15 – 19,* 1997. *Chia Laguna, Sardenga, Italy*. Abstracts. p. 61
111. Nemoshkalenko V V et al. *Amorfnye Metallicheskie Splavy* (Amorphous Metallic Alloys) (Kiev: Naukova Dumka, 1987)
112. Itoh F et al. *Nucl. Instrum. Methods Phys. Res.* **199** (1/2) 323 (1982)
113. Vehanen A et al. *Phys. Rev. B* **29** 2371 (1984)
114. Kristiak J, in *9th Int. Conf. on Rapidly Quenched and Metastable Materials* (*RQ9*). *Bratislava, Aug. 25 – 30, 1996*. Book of Abstracts, p. 9
115. Limoge Y *Mater. Sci. Forum.* **15/18** 517 (1987)
116. Akhtar D, Misra R D K *Scr. Metall.* **19** 1195 (1985)
117. De Hey P, Sietsma J, van den Beukel A, in *9th Int. Conf. on Rapidly Quenched and Metastable Materials* (*RQ9*). *Bratislava, Aug. 25 – 30, 1996*. Book of Abstracts, p. 180
118. Kajcsos Zs et al., in *Proc. 6th Int. Conf. Positron Annihilation, Arlington, 1982* p. 601
119. Gleser A M, Betehtin V I, in *9th Int. Conf. on Rapidly Quenched and Metastable Materials* (*RQ9*). *Bratislava, Aug. 25 – 30, 1996*. Book of Abstracts, p. 176
120. Ahmadzadeh M, Cantor B *J. Non-Cryst. Solids* **43** 189 (1981)
121. Finney J L *Proc. R. Soc. London Ser. A* **319** 479 (1970)
122. Belashchenko D K *Rasplavy* **1** (3) 45 (1987)
123. Fam Khak Huang, Belashchenko D K *Izv. Vyssh. Uchebn. Zaved. Chernaya Metallurgiya* (5) 91 (1987)
124. Belashchenko D K, Golubenkova S V *Izv. Akad. Nauk SSSR Metally* (2) 177 (1991)
125. Belashchenko D K, Gritsenko A B *Izv. Vyssh. Uchebn. Zaved. Chernaya Metallurgiya* (7) 102 (1985)
126. Fam Khak Huang et al. *Izv. Akad Nauk SSSR Metally* (2) 118 (1998)
127. Van Ee L D, Thijsse B J, Sietsma J, in *7th Int. Conf.on the Structure of Non-Crystalline Materials* (*NCM7*). *September 15 – 19, 1997. Chia Laguna, Sardenga, Italy*. Abstracts, p. 14
128. Fam Khak Huang, Belashchenko D K, Nguen Suan Tu *Izv. Vyssh. Uchebn. Zaved. Chernaya Metallurgiya* (7) 172 (1987)
129. Schuehmacher J J, Guiraldenq P *Acta Metall.* **31** 2043 (1983)
130. Valenta P et al. *Phys. Status Solidi B* **106** (1) 129 (1981)
131. Frost H J *Acta Metall.* **30** 889 (1982)
132. Medvedev N N, Naberukhin Yu I *Zh. Struct. Khim.* **28** (3) 117 (1987)
133. Naberukhin Yu I, Voloshin V P, Medvedev N N *Zh. Fiz. Khim.* **66** 155 (1992) [*Russ. J. Phys. Chem.* **66** 81 (1992)]
134. Medvedev N N *Dokl. Ross. Akad. Nauk* **337** 767 (1994)
135. Belashchenko D K, Fam Khak Huang *Izv. Vyssh. Uchebn. Zaved. Chernaya Metallurgiya* (5) 165 (1981)
136. Delaye J M, Limoge Y *Diffus. Defect Data A* **95 – 98** (Pt. 2) 1181 (1993)
137. Delaye J M, Limoge Y *J. Phys. I* (Paris) **3** 2063 (1993)
138. Delaye J M, Limoge Y *J. Phys. I* (Paris) **3** 2079 (1993)
139. Frank W, Gustin W, Horz M, in *Liquid and Amorphous Metals. 9th Int. Conf. Chicago, USA, Aug. 27 – Sept. 1 1995*. Theses, p. 75
140. Chan S L, Elliott S R *Phys. Rev. B.* **43** 4423 (1991)

141. Mitra S K *Philos. Mag. B* **45** 529 (1982)
142. Taraskin S N, Elliott S R, Klinger M I *J. Non-Cryst. Solids* **192–193** 263 (1995)
143. Lee J H, Elliott S R *J. Non-Cryst. Solids* **192–193** 133 (1995)
144. Hirao K, Soga N *J. Non-Cryst. Solids* **84** 61 (1986)
145. Soules T *J. Non-Cryst. Solids* **49** 29 (1982)
146. Balasubramanian S, Rao K J *J. Chem. Phys.* **97** 8835 (1993)
147. Huang Chengde, Cormack A N "Phys. Non-Cryst. Solids", in *7th Int. Conf., Cambridge, Aug. 4–9, 1991. London; Washington* (*DC*), 1992, p. 31
148. Yap A, Elliott S R, in *6th Int. Conf. on the Structure of Non-Crystalline Materials* (*NCM6*). *Praha, Aug. 29–Sept. 2 1994*. Abstracts, p. 241
149. Belashchenko D K, Sapozhnikova S Yu *Zh. Fiz. Khim.* **71** 1036 (1997) [*Russ. J. Phys. Chem.* **71** 920 (1997)]
150. Belashchenko D K, Sapozhnikova S Yu *Neorg. Mater.* **33** 822 (1997) [*Inorganic Mater.* **33** 692 (1997)]